

Nocturnal HR Slope Signatures Differentiate Sleep Quality Phenotypes, A Topological Approach

Federico Starace

May 21, 2025

Contents

1 Abstract	5
2 Introduction	6
2.1 Background	6
2.2 Chronotype	6
2.2.1 Chronotype Measurement Methods	7
2.2.2 Types of Chronotypes (Morning-Type, Evening-Type, Neither-Type)	10
2.2.3 Biological Influences on Chronotype (Age, Sex, Genetics) . .	12
2.2.4 Social Jet Lag	14
2.3 Sleep Architecture	17
2.3.1 N1 Stage (Light Sleep)	17
2.3.2 N2 Stage (Intermediate Sleep)	18
2.3.3 N3 Stage (Deep Sleep)	18
2.3.4 REM Stage (Rapid Eye Movement Sleep)	18
2.3.5 Arousals and Micro-Awakenings	18
2.4 Neurophysiology of Sleep	18
2.5 Sleep Regulation: Homeostatic and Circadian Control	22
2.6 Circadian Rhythms: The Body's Internal Clock	24
2.7 The Autonomic Nervous System (ANS)	26
2.8 ANS Activity During Sleep	28
2.9 Interaction of Sleep and Circadian Rhythms on ANS	30
2.10 Factors Influencing Sleep, Circadian Rhythms, and ANS	32
2.11 Measuring Sleep and ANS Activity: From PSG to Wearables . . .	36
2.12 Sleep indices	40
2.12.1 Sleep Duration (SD)	40
2.12.2 Wake After Sleep Onset (WASO)	40
2.12.3 Total Sleep Time (TST)	40
2.12.4 Sleep Efficiency (SE)	40
2.12.5 Sleep Onset Latency (SOL)	40
2.12.6 Sleep Stage Distribution (SSD)	40
2.12.7 Sleep Regularity Index (SRI)	41
2.12.8 Mid Sleep Point (MSP)	41
2.12.9 Number of Awakenings (NAw)	42
2.12.10 Activity Index (ActI)	42
2.12.11 Movement Index (MovI)	43
2.12.12 Fragmentation Index (FI)	43
2.12.13 Sleep Fragmentation Index (SFI)	43
2.12.14 Apnea Hypopnea Index (AHI)	43

2.13	Chronobiometrical Analysis of Sleep	44
2.13.1	Period	44
2.13.2	Mesor	44
2.13.3	Amplitude	44
2.13.4	Acrophase	45
2.13.5	Phase	45
3	Materials	46
3.1	Software Environment	46
3.2	Data Collection	46
4	Methods	47
4.1	Experimental Protocol	47
4.1.1	Preprocessing	47
4.1.2	Feature Extraction Pipeline Step	47
4.1.3	Dimensionality Reduction and Clustering	49
4.1.4	Subject-Level Cluster Consistency and Analysis	51
4.1.5	Causal Inference and Confounder Adjustment	52
4.1.6	Statistical Modeling and Visualization	53
4.1.7	Parameter Tuning via Grid Search	54
5	Results	56
5.1	Study Population Characteristics	56
5.2	Clustering Outcome and Phenotype Identification	56
5.3	Cluster Characterization	58
5.4	Heart Rate, Chronotype, and Sleep Index Interactions	62
5.5	Individual-Level Consistency	64
5.6	Statistical Modeling of Cluster Membership	65
5.7	Summary of Results	67
6	Discussion	69
6.1	Heart Rate Trend as a Sleep Phenotype Predictor	69
6.2	Topological Data Analysis in Sleep Research and Study Limitations	70
6.3	Summary of Principal Findings	71
6.4	Interpretation of Findings	72
6.5	Limitations of the Study	73
6.6	Future Research Directions	73
6.7	Conclusion	74

7 Appendix	75
7.1 Online Material	75
7.2 Supplementary Figures and Tables	75
7.2.1 Clustering Parameters	75
7.2.2 Overall Clustering Statistics	76
7.2.3 Heart Rate Statistics by Cluster	76
7.2.4 Individual Cluster Heart Rate Profiles	77
7.2.5 Detailed Cluster Statistics	77
8 Acknowledgements	83
References	84

1 Abstract

This study aimed to identify distinct sleep phenotypes based on heart rate (HR) dynamics during sleep and to investigate their associations with demographic and sleep-related factors using a causal inference framework. We analyzed 5040 sleep episodes from 870 healthy adults (18-75 years), collected via the Sleepacta platform using Fitbit HR devices. The analytical pipeline involved preprocessing of HR time series, feature extraction including Topological Data Analysis (TDA) of HR slopes (persistence entropy) and HR nadir timing characteristics, dimensionality reduction using UMAP, and KMeans clustering with optimal cluster number selection via Silhouette analysis. Subject-level cluster consistency and Bayesian multinomial mixed-effects models, guided by a Directed Acyclic Graph (DAG) for confounder adjustment, were employed for statistical analysis.

The clustering approach, primarily driven by weighted HR nadir timing, identified three distinct phenotypes: Cluster 0 ("Seahorse-like," 35.0%, mid-period nadir), Cluster 1 ("Sliding Slope," 38.2%, late nadir), and Cluster 2 ("Symmetric Hammock," 26.9%, early nadir). These phenotypes significantly differed in nadir timing percentage ($p < 0.0001$), mean/nadir HR, age, sex distribution, Sleep Fragmentation Index (SFI), individual chronotype, absolute chronotype desynchronization, and Wake After Sleep Onset (WASO) (all $p < 0.05$). However, intra-individual consistency in exhibiting a specific phenotype was low (mean consistency score = 0.17). After causal adjustment, Bayesian modeling revealed significant predictors of phenotype membership, including individual chronotype, age, sex, absolute chronotype desynchronization, Sleep Regularity Index (SRI), and Sleep Efficiency (SE).

This research demonstrates that HR nadir timing is a key differentiator of nocturnal HR patterns, yielding distinct phenotypes associated with various demographic and sleep characteristics. The low intra-individual consistency highlights substantial nightly variability in HR dynamics. These findings underscore the complexity of HR regulation during sleep and provide a robust methodological framework for future investigations into HR-based sleep phenotyping, particularly regarding the interplay between trait-like predispositions and state-dependent nightly variations.

2 Introduction

2.1 Background

Sleep is increasingly understood to be an active biological process that is fundamental to human health and brain function, rather than merely a passive state of rest . Insufficient or irregular sleep is associated with higher all-cause mortality and an elevated risk of numerous chronic diseases (Zheng et al., 2024). In particular, healthy sleep patterns correlate with lower incidence of obesity, cardiometabolic disorders, and even reduced susceptibility to infectious illness (Zheng et al., 2024; Li et al., 2025). During sleep, the body carries out critical restorative tasks including regulating hormones, maintaining metabolic balance, bolstering immune defenses, and clearing neurotoxic waste from the brain via the glymphatic system (Xie et al., 2013). Sleep is also crucial for cognitive performance, as it allows the brain to consolidate memories and restore learning capacity; indeed, memory consolidation critically relies on sleep, especially during deep slow-wave sleep (Mittermaier et al., 2024). Similarly, sleep plays a key role in emotional regulation: sufficient sleep fosters stable mood, whereas sleep deprivation amplifies emotional reactivity. For instance, experimentally disrupting rapid eye movement (REM) sleep causes a spike in next-day negative affect accompanied by heightened amygdala activity (Glosemeyer et al., 2020), and chronic sleep deficits are linked to increased risk of depression and anxiety disorders (Zheng et al., 2024).

2.2 Chronotype

Chronotype refers to an individual's natural inclination for sleep-wake timing, often described as "morningness" or "eveningness." It reflects the alignment of one's internal circadian clock with the 24-hour day-night cycle, influencing peak alertness times and preferred sleep schedules (Roenneberg et al., 2003). In adult populations, chronotype varies widely - some people naturally wake and function best at early hours ("larks" or morning types), while others feel more energetic later and prefer late sleep ("owls" or evening types), with many falling in between as intermediates. Chronotype is not merely a preference; it has biological underpinnings and significant implications for health, work performance, and well-being (Roenneberg et al., 2003; Jankowski et al., 2019). This report provides a comprehensive, thesis-style overview of chronotype in adults, covering how it is measured, the types and distribution of chronotypes, biological influences (age, sex, and genetics), the phenomenon of social jet lag, effects of seasonality and light exposure, links to sleep disorders, and associations with autonomic functions.

2.2.1 Chronotype Measurement Methods

Accurately measuring chronotype is crucial for research and clinical applications. Methods range from objective biological markers to subjective self-report questionnaires, each with advantages and limitations in terms of reliability, validity, and feasibility for large studies:

Dim Light Melatonin Onset (DLMO) DLMO is considered the gold-standard marker of internal circadian timing (Pandi-Perumal et al., 2007; Burgess et al., 2018). It is defined as the time in the evening when the pineal gland begins secreting melatonin under dim light conditions, typically occurring 2-3 hours before habitual sleep onset (Pandi-Perumal et al., 2007). Because melatonin release is tightly controlled by the central clock (SCN), DLMO provides a direct physiological measure of a person's circadian phase. DLMO is highly reliable within individuals under controlled conditions, showing consistent timing on repeat measurements, and it strongly correlates with core body temperature rhythms and other circadian markers (Pandi-Perumal et al., 2007). However, using DLMO in population studies is challenging - it requires collecting multiple saliva or blood samples in dim-light settings, which is invasive, labor-intensive, and costly (Reiter et al., 2021). This makes DLMO impractical for very large or epidemiological samples. In small lab-based studies, DLMO is invaluable, but in large-scale research, it's often reserved as a validation tool rather than a primary measure. Notably, studies comparing DLMO to questionnaire-based chronotype measures find only moderate correlations (r on the order of 0.3-0.6) (Burgess et al., 2018), indicating that while related, self-reported "morningness-eveningness" only partly predicts actual circadian phase. For example, one study found DLMO correlated with MEQ score at $r = -0.25$ and with MCTQ-derived midpoint at $r = 0.32$ (Reiter et al., 2021), reflecting significant but not perfect correspondence. In sum, DLMO offers high validity as a circadian phase marker, but limited applicability in large populations due to practical constraints.

Morningness-Eveningness Questionnaire (MEQ) and rMEQ The Horne-Östberg Morningness-Eveningness Questionnaire (MEQ) is a classic self-assessment tool introduced in 1976 to determine whether a person is a "morning" or "evening" type. The full MEQ consists of 19 questions about preferred wake and bed times, alertness, and activity timing preferences (Horne and Ostberg, 1976). It yields a score ranging roughly from 16 (extreme evening) to 86 (extreme morning), with higher scores indicating greater morningness. The MEQ has been extensively validated; originally it was even cross-validated against circadian body temperature rhythms (finding that morning types had earlier daily temperature peaks) (Horne and Ostberg, 1976). It shows high internal consistency and test-retest reliability

(often Cronbach's $\alpha > 0.80$) (Di Milia et al., 2013). For large surveys, a reduced MEQ (rMEQ) was developed - a shorter questionnaire (commonly 5 items) derived from the MEQ. The rMEQ provides a quicker assessment of chronotype while maintaining good psychometric properties. Studies indicate the rMEQ is highly correlated with the full MEQ (and the related Composite Scale of Morningness) since they share many questions, reflecting that it captures the same underlying construct (Di Milia et al., 2013). Its reliability is "satisfactory" (slightly lower than the full MEQ due to fewer items, but still robust) (Di Milia et al., 2013). In terms of validity, MEQ and rMEQ scores show expected associations with external criteria: for instance, extreme morning types by MEQ have earlier melatonin and temperature rhythms than extreme evening types (Di Milia et al., 2013). These questionnaires are cheap and easy to administer to thousands of people, making them excellent for population studies. One limitation is that they measure self-reported preference (diurnal preference) more than actual behavior or physiology. Nevertheless, their widespread use and strong reliability make them a staple for chronotype research in large cohorts.

Munich Chronotype Questionnaire (MCTQ) The MCTQ, developed by Roenneberg et al., 2003, takes a different approach by focusing on actual sleep timing behavior rather than subjective preference. It collects detailed self-reports of an individual's typical sleep and wake times on workdays versus free days, from which one can calculate the person's chronotype as the midpoint of sleep on free days (often corrected for "oversleep" if a person accumulates sleep debt on weekdays). The corrected mid-sleep (MSF_{sc}) accounts for any shift due to catching up on sleep, providing a better estimate of the intrinsic phase of sleep timing. The MCTQ yields a continuous chronotype measure in local clock time (e.g. a person's MSF_{sc} might be 3:45 AM). Because it quantifies behavior, it can capture small differences between individuals that questionnaires like the MEQ (which output a coarse score/category) might not. The MCTQ is not a singular "scale" with a total score, so traditional reliability coefficients don't directly apply (Suh et al., 2017; Roenneberg, 2023). However, it has shown good construct validity: MCTQ-derived chronotype correlates moderately with MEQ scores and more strongly with physiological markers. Studies report that MSF_{sc} correlates with DLMO timing (Spearman $r = 0.54\text{-}0.68$ in some samples), a higher correlation than typically seen with MEQ ($r = -0.4 \text{ to } -0.5$) (Burgess et al., 2018). This suggests MCTQ's behavioral measure may better approximate internal clock phase than preference scores do. In large-scale surveys (tens of thousands of respondents worldwide), the MCTQ has proven highly applicable, revealing patterns of chronotype distribution by age, sex, and latitude (discussed later). Its simplicity (an online or paper form) and focus on actual sleep times make it a powerful tool for epidemiological research. One

must note, however, that defining chronotype categories from MCTQ (e.g. what counts as "evening type" vs "morning") is less standardized - researchers often split the continuous MSF_{sc} data into tertiles or percentiles to create groups (Suh et al., 2017; Roenneberg, 2023; Wei et al., 2024). Despite this, MCTQ has become a cornerstone for chronobiology studies, especially in conjunction with concepts like social jetlag derived from the same data. From the MCTQ, we can derive the following parameters:

- SD_f Sleep Duration on free days

$$SD_f = \frac{1}{n_f} \sum_{i \in F} SD_i \quad \text{where } F \text{ is the set of free days and } n_f \text{ is the number of free days} \quad (1)$$

- SD_w Sleep Duration on work days

$$SD_w = \frac{1}{n_w} \sum_{i \in W} SD_i \quad \text{where } W \text{ is the set of work days and } n_w \text{ is the number of work days} \quad (2)$$

- SD_{week} Average Weekly Sleep Duration

$$SD_{week} = \frac{SD_f \times n_f + SD_w \times n_w}{n_f + n_w} \quad (3)$$

- MSF Average Mid Sleep Point on free days

$$MSF = \frac{1}{n_f} \sum_{i \in F} MSP_i \quad \text{where } F \text{ is the set of free days and } n_f \text{ is the number of free days} \quad (4)$$

- MSW Average Mid Sleep Point on work days

$$MSW = \frac{1}{n_w} \sum_{i \in W} MSP_i \quad \text{where } W \text{ is the set of work days and } n_w \text{ is the number of work days} \quad (5)$$

- MSF_{sc} Mid-sleep time on free days corrected for sleep debt on work days

$$MSF_{sc} = \begin{cases} MSF & \text{if } SD_f \leq SD_w \\ MSF - \frac{SD_f - SD_{week}}{2} & \text{if } SD_f > SD_w \end{cases} \quad (6)$$

- SJL_{rel} Social Jet Lag (relative)

$$SJL_{rel} = MSF - MSW \quad (7)$$

- SJL_{abs} Social Jet Lag (absolute)

$$SJL_{abs} = |MSF - MSW| \quad (8)$$

Actigraphy Actigraphy offers an objective method for assessing sleep-activity patterns over extended periods, typically using wrist-worn devices that measure movement. For chronotype assessment, actigraphy-derived parameters such as the average midpoint of sleep across all recorded days (aMS-acti), or features derived from cosinor analysis (e.g., acrophase) or non-parametric methods (e.g., L5-mid, the midpoint of the least active 5 hours), can be utilized (Wei et al., 2024). These objective measures of rest-activity rhythms can complement subjective questionnaire data by providing insights into actual sleep timing and consistency in an individual's natural environment. Studies have shown that actigraphy-derived chronotype measures can correlate with questionnaire-based assessments like the MEQ and MCTQ, though the strength of correlation can vary depending on the specific actigraphic parameter used and the duration of the recording (Wei et al., 2024; Schneider et al., 2022). For instance, Wei et al., 2024 found that a simple average midpoint of sleep from actigraphy (aMS-acti) performed well in terms of consistency with subjective chronotype, test-retest reliability, and external validity in young adults over a 5-day recording period. Schneider et al. (2022) suggested that longer recording periods (e.g., 3 weeks) might be needed for more stable actigraphy-based chronotype estimations. While actigraphy does not measure circadian phase directly (like DLMO), it provides valuable objective data on behavioral rhythms, making it suitable for large-scale studies and situations where long-term, unobtrusive monitoring of chronotype is desired.

In summary, DLMO offers high physiological validity but is impractical outside small studies (Reiter et al., 2021); questionnaires (MEQ/rMEQ) provide reliable and valid self-assessment of circadian preference, ideal for large populations; and the MCTQ captures behavioral manifestation of chronotype with fine granularity, bridging the gap between subjective preference and objective circadian phase (Burgess et al., 2018). Often, researchers will use questionnaires to screen or categorize chronotype in large samples and reserve DLMO measurements for validation in a sub-sample or in clinical research. All methods have been key in advancing our understanding of how chronotype varies and why it matters in adult populations.

2.2.2 Types of Chronotypes (Morning-Type, Evening-Type, Neither-Type)

Chronotype exists on a continuum from very early to very late types, but for practical purposes it's often classified into broad categories. The most common classification recognizes morning-types, intermediate-types, and evening-types. Morning types ("larks") naturally wake early, feel most alert in the morning, and prefer to sleep earlier in the evening; evening types ("owls") wake later and are most energized later in the day, preferring late bedtimes; intermediates fall in between

these extremes. In population studies, chronotype (e.g. measured by mid-sleep or questionnaires) shows an approximately normal (Gaussian) distribution -most adults are intermediate, with fewer people at the extreme early or extreme late ends (Fischer et al., 2017). Figure 1 below illustrates a typical distribution of chronotypes in a large sample of 53,000 adults (using mid-sleep on free days as the chronotype indicator): the peak of the curve represents the "middle-of-the-road" chronotypes, while the tails represent the rare extreme larks and owls.

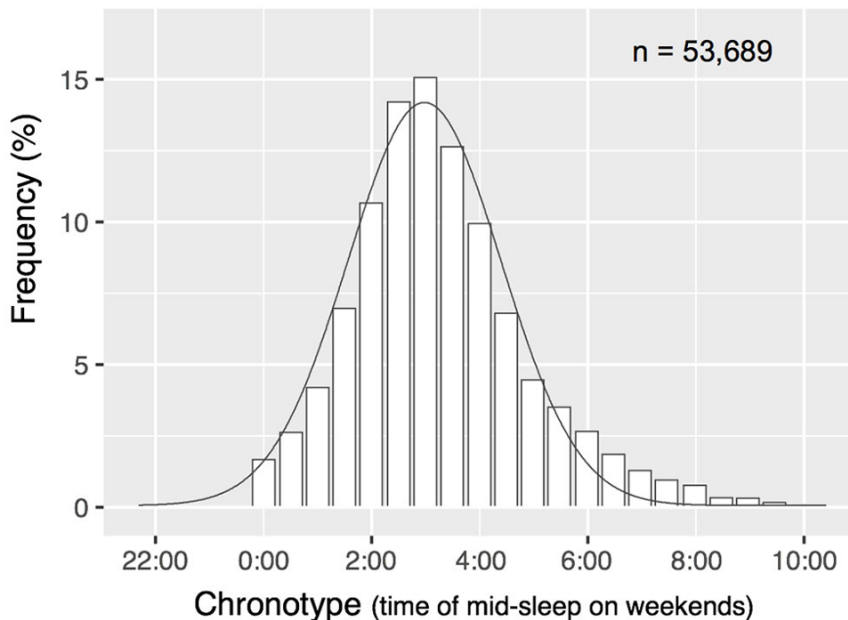


Figure 1: Distribution of chronotype (mid-sleep on free days) in 53k U.S. adults, showing a bell curve spanning 12 hours between extreme morning and extreme evening types. Most people cluster near the center (e.g. mid-sleep around 3-5 AM), with only a small percentage having very early or very late chronotypes (Fischer et al., 2017).

To define chronotype groups, researchers often use score cutoffs on questionnaires. For instance, the rMEQ can be interpreted as follows based on Natale et al., 2006: **E-type (Evening type):** rMEQ score 4-11; **N-type (Neither type):** rMEQ score 12-17; **M-type (Morning type):** rMEQ score 18-25. These categories provide convenient labels, though the underlying chronotype is continuous. The N-type (neither morning nor evening) is the most common in adult populations - they don't have a pronounced preference and usually adapt more easily to standard work schedules.

2.2.3 Biological Influences on Chronotype (Age, Sex, Genetics)

Chronotype is shaped by inherent biological factors as well as environment. Two of the most influential biological factors in adults are age and sex, which both drive notable differences in circadian timing. Additionally, genetic background plays a role by determining one's baseline clock speed and sensitivity to light cues.

Age and Chronotype Human chronotype undergoes predictable shifts across the lifespan. During adolescence, there is a well-documented trend toward later chronotypes - teenagers generally become "night owls" compared to young children. This evening shift peaks in the late teens or early twenties: large-scale data show that chronotype is latest around age 19-20 on average, after which it gradually shifts earlier (more morning) with advancing age (Roenneberg et al., 2007). For example, a U.S. survey of 53,000 people found the average mid-sleep chronotype at age 17-18 was about 4:30 AM, whereas by age 60 it was around 3:00 AM (indicating earlier sleep timing in older adults) (Fischer et al., 2017). After about age 20, each subsequent decade of life is associated with somewhat earlier wake and bedtimes on average. In practical terms, younger adults (20s-30s) tend to be later chronotypes than middle-aged adults, and older adults (60s and beyond) are often strongly morning-oriented. The variability in chronotype also decreases with age - adolescents and young adults show a wide spread of chronotypes, whereas among seniors, most people are relatively early and the extreme late chronotypes become rare (Fischer et al., 2017; Roenneberg et al., 2007). This age-related pattern is so robust that researchers have dubbed the peak-late chronotype in early adulthood as a "marker of the end of adolescence" (Roenneberg et al., 2007). The shifts are partly driven by biological maturation and possibly hormone changes; for instance, the surge of sex hormones in puberty correlates with the delay in circadian phase, and in later life changes like menopause or general aging of the suprachiasmatic nucleus (master clock) may contribute to advancing chronotype. In summary, age has a major influence: most people will find their sleep schedule naturally moves earlier as they transition from young adulthood to older age (Roenneberg et al., 2007), even without external pressures.

Sex Differences Sex (or gender) also influences chronotype, though the effect is more subtle than that of age. Generally, studies have found that men are slightly more evening-oriented than women on average, at least up until mid-life (Roenneberg et al., 2007). A comprehensive meta-analysis covering 186,000 individuals concluded that men had a later chronotype than women with a small effect size (standardized mean difference -0.07, indicating men being more "evening") (Randler and Engelke, 2019). The difference is most pronounced in young adults - for example, between ages 15-30, males tend to reach peak lateness slightly later and

have a greater proportion of "owls" than females of the same age. Interestingly, these gender differences diminish and even reverse with age. By the time adults reach around 50-60 years old, women may become slightly more evening-oriented than men of the same age (Randler and Engelke, 2019). In other words, young women are generally more morning type than young men, but older women are less morning type than older men. The meta-analysis predicted the chronotype gap flips as mean age increases, suggesting hormonal or lifestyle factors over the lifespan (for instance, pregnancy, child-rearing, menopause in women; differences in employment or retirement patterns in older men) might shift these tendencies. It's also worth noting that variability in chronotype has been observed to be higher in men than in women at younger ages (Steven et al., 2017) - perhaps reflecting that more men occupy the extreme late end of the distribution in youth. By older adulthood, both sexes converge toward morningness. Overall, sex contributes a modest but measurable influence on chronotype in adults, interacting with age. Contemporary large studies (including international samples) consistently find this pattern: a young male bias toward eveningness that wanes with age (Randler and Engelke, 2019).

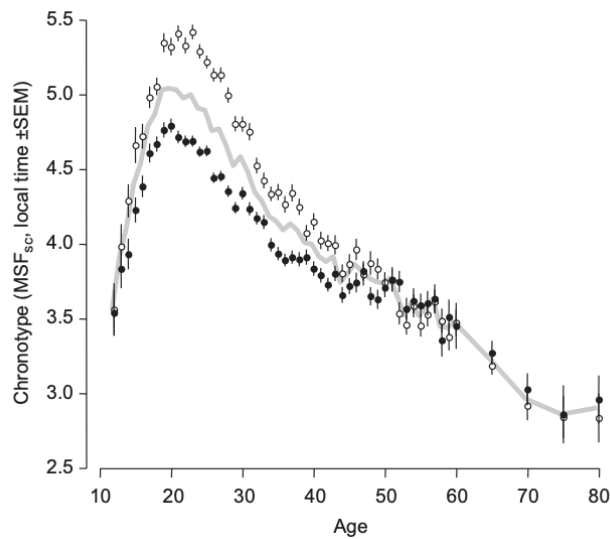


Figure 2: Age, Sex and Chronotype (filled circles, females; open circles, males; the grey line shows the averages for the entire population) Roenneberg et al., 2003

Genetic Factors Underlying one's chronotype is a genetic component - essentially, "clock genes" and other genetic variants can predispose individuals to different circadian timing. Twin and family studies estimate that roughly 30-50% of the variance in chronotype is heritable (McCall et al., 2021). This means about

half of what makes one person a morning lark and another a night owl can be traced to genetic differences. Indeed, researchers have identified numerous gene polymorphisms associated with morningness-eveningness. For example, certain variants of the genes PER1, PER2, PER3, CRY1, CLOCK and others have been linked to shifted sleep timing. Large genome-wide association studies (including hundreds of thousands of people) have uncovered dozens of loci related to self-reported morningness (Kalmbach et al., 2016) - each variant typically has a small effect, but collectively they influence a person's chronotype. Rare mutations can have dramatic effects: for instance, a mutation in the gene PER2 was found to cause Familial Advanced Sleep Phase Syndrome (extreme early chronotype) in one family (Pavithra et al., 2024). However, such single-gene circadian disorders are rare; for most individuals, chronotype arises from the combined influence of many genes plus environmental factors. In adults, genetics set the propensity for being more morning or evening, but environment (light exposure, work schedule, etc.) can modulate the expression of that tendency (Kalmbach et al., 2016).

2.2.4 Social Jet Lag

Modern life often forces people to live on a schedule that conflicts with their internal circadian time. Social jet lag (SJL) refers to this misalignment - it is the discrepancy between one's biological clock and one's social obligations (work, school, etc.) (Roenneberg, 2023). Essentially, it's like being perpetually "jetlagged" not by crossing time zones, but by the weekly cycle of workdays and free days. A common way to quantify social jet lag is by comparing the midpoint of sleep on workdays (when one must often rise at a set time by alarm) with the midpoint of sleep on free days (when one sleeps based on their natural preference). The greater the gap, the more social jet lag a person has. For example, an evening-type individual might have to wake at 6 AM for work (mid-sleep perhaps 3 AM on workdays), but on weekends they sleep in and their mid-sleep is 5 AM - this 2-hour difference is social jet lag. Figure 3 below illustrates this concept: the top bar shows a late chronotype forced to sleep earlier on workdays (orange bar) than they naturally would on free days (green bar), resulting in a misalignment equal to the horizontal arrow (SJL) (Jankowski, 2017 Wittmann et al., 2006). The bottom bar shows an approach to correct for sleep debt (since many people accrue sleep loss on workdays and oversleep on free days), but the fundamental idea is the same - social jet lag is the wedge between socially imposed timing and biological timing.

In industrialized societies, social jet lag is extremely common - about two-thirds of working or studying adults experience significant SJL on a regular basis. Many people effectively live in "two time zones": one for the work week and one for the weekend. Evening-type adults are most prone, because work/school schedules tend to start early, forcing night owls to truncate sleep on weekdays. These individuals

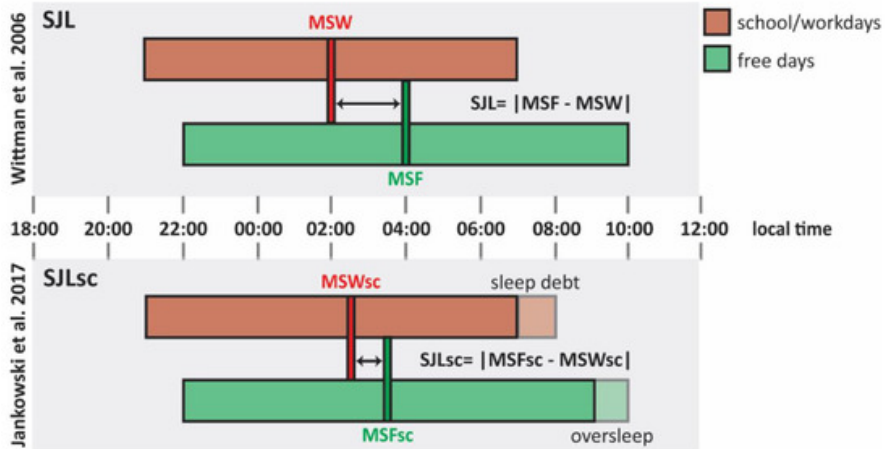


Figure 3: Illustration of social jet lag. In this example, a late chronotype's sleep period (green bar) is much later on free days than on workdays (orange bar). MSW = midsleep on workdays, MSF = midsleep on free days. The difference (black arrow) is the social jet lag (SJL) due to work obligations causing a shift from the person's natural schedule Jankowski, 2017 Wittmann et al., 2006

often compensate by sleeping in later on days off, which can lead to 2+ hours of SJL each week. Even morning types can have some social jet lag if they work irregular shifts or over-extend their weekday schedule. Essentially, millions of adults "jetlag" themselves every weekend by switching to a more natural late schedule and then dragging back to an earlier alarm schedule by Monday. The health and lifestyle impacts of social jet lag are an active area of research - and they are concerning. Chronic circadian misalignment (like ongoing SJL) has been linked to a variety of negative outcomes. Physiologically, social jet lag is associated with increased risks of metabolic disorders: studies have found that greater SJL correlates with higher likelihood of obesity, insulin resistance, and metabolic syndrome (Caliandro et al., 2021). For instance, one large epidemiological study reported that individuals with more than 2 hours of SJL had significantly higher body mass index (BMI) and doubled risk of being overweight, independent of total sleep duration (Caliandro et al., 2021). Another cohort (the New Hoorn Study in the Netherlands) found that about 2 hours of social jet lag was linked to a two-fold increase in risk for pre-diabetes and Type 2 diabetes (Koopman et al., 2017). The underlying reason is thought to be circadian misalignment's effect on hormonal regulation - when eating, activity, and sleeping times are inconsistent with our internal clock, metabolism suffers. Social jet lag has also been tied to cardiovascular risks: people with higher SJL show worse profiles of triglycerides and cholesterol, and some data suggest higher rates of heart disease in late chronotypes which might be mediated by

years of circadian misalignment. Beyond physical health, mental health can be affected. Social jet lag and large discrepancies in sleep timing have been associated with increased depression symptoms and lower subjective well-being (Koopman et al., 2017). For example, a study in a rural population found higher depression scores in those with greater SJL and later chronotype (Caliandro et al., 2021). Fatigue, low mood, and cognitive dulling are common complaints when one's social schedule fights their biological clock. Lifestyle factors often interplay with social jet lag as both cause and effect. Adults experiencing heavy SJL might resort to stimulants like caffeine to wake up (which can further disrupt sleep later) and then need relaxation aids or sedatives to sleep at imposed times. Unhealthy eating patterns are another consequence: research noted that those with more social jet lag tend to eat more irregularly and have higher consumption of sugary/fatty foods, possibly due to circadian-driven appetite changes or convenience eating at odd hours (Shafer et al., 2023). Social habits, like late-night socializing on weekends, can exacerbate the cycle, creating a vicious circle of weekday sleep restriction and weekend oversleep. Importantly, social jet lag is not a trivial inconvenience - it is increasingly recognized as a public health concern. Because such a large portion of the adult population lives with some degree of mismatch (especially those with evening chronotypes doing early jobs), the aggregate impact on health and productivity is significant. There is interest in societal interventions such as more flexible work hours or later school start times to mitigate social jet lag. Some companies have experimented with allowing employees to start later if they are night owls. Aligning one's schedule more closely to their chronotype - when possible - or keeping a more consistent sleep routine even on free days can reduce social jet lag. In conclusion, social jet lag encapsulates the tension between biological time and social time. It is highly prevalent among adults and has measurable impacts on metabolic, cardiovascular, and mental health. Addressing SJL is a challenge, as it often requires changes at both the individual level (sleep hygiene, consistency) and societal level (workplace and institutional flexibility). Nonetheless, recognizing the concept of social jet lag is the first step for many adults to understand their own fatigue and health issues in the context of circadian alignment.

2.3 Sleep Architecture

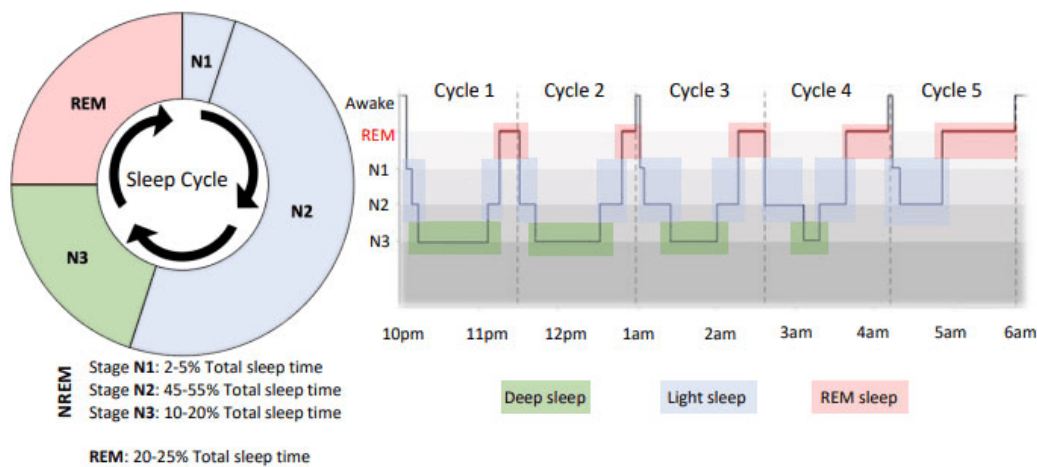


Figure 4: Sleep architecture Driller et al., 2023

The sleep cycle is a series of stages that occur during sleep, including non-rapid eye movement (NREM) and rapid eye movement (REM) sleep. NREM sleep consists of three stages: N1 (light sleep), N2 (intermediate sleep), and N3 (deep sleep or slow-wave sleep). Each stage serves distinct physiological functions, with N3 being particularly important for physical restoration and REM sleep crucial for cognitive processes and emotional regulation. A typical night involves 4-6 cycles of alternating NREM and REM sleep, with each cycle lasting approximately 90-120 minutes.

2.3.1 N1 Stage (Light Sleep)

N1, or Stage 1 sleep, is the lightest stage of non-REM sleep and serves as a transition between wakefulness and deeper sleep stages. During this stage, brain waves begin to slow from the beta waves of wakefulness to alpha waves and then to theta waves. Characterized by slow eye movements, decreased muscle activity, and occasional muscle twitches or hypnic jerks, N1 typically comprises 2-5% of total sleep time in healthy adults. People in N1 sleep can be easily awakened and may not even perceive they were asleep. This stage is often experienced during brief naps or during sleep onset, playing a crucial role in the initial descent into deeper sleep stages.

2.3.2 N2 Stage (Intermediate Sleep)

N2, or Stage 2 sleep, is the second stage of non-REM sleep and is characterized by a more pronounced slowing of brain waves compared to N1. This stage is marked by the presence of sleep spindles and K-complexes, which are high-frequency, low-amplitude waves that are associated with memory consolidation and learning. N2 typically comprises 45-55% of total sleep time in healthy adults.

2.3.3 N3 Stage (Deep Sleep)

N3, or Stage 3 sleep, is the deepest stage of non-REM sleep and is characterized by slow delta waves. This stage is crucial for physical restoration, as it promotes growth hormone secretion and tissue repair. N3 typically comprises 20-25% of total sleep time in healthy adults.

2.3.4 REM Stage (Rapid Eye Movement Sleep)

REM sleep is the fourth and final stage of the sleep cycle. It is characterized by rapid eye movements, increased brain activity, and vivid dreaming. REM sleep is crucial for memory consolidation and emotional regulation. It typically comprises 20-25% of total sleep time in healthy adults.

2.3.5 Arousal and Micro-Awakenings

Arousal are brief awakenings from sleep, typically lasting less than 30 seconds. Micro-awakenings are even briefer awakenings, lasting less than 10 seconds. Arousal and micro-awakenings can disrupt sleep continuity and affect sleep quality.

2.4 Neurophysiology of Sleep

The sleep-wake cycle, characterized by the intricate alternation of non-rapid eye movement (NREM) and rapid eye movement (REM) sleep stages, is an active and highly organized neurophysiological process, far from being a mere passive state of rest (Morris et al., 2012). Its sophisticated regulation arises from complex interactions between a network of brain regions, a diverse array of neurotransmitters, and precisely orchestrated neural circuits, primarily located within the hypothalamus, brainstem, and forebrain.

A central tenet in understanding sleep-wake transitions is the “flip-flop switch” model, which posits a mutually inhibitory relationship between sleep-promoting neurons, predominantly found in the ventrolateral preoptic nucleus (VLPO) of the hypothalamus, and the wake-promoting nuclei of the ascending reticular activating

system (ARAS) (Morris et al., 2012). The VLPO, utilizing inhibitory neurotransmitters such as GABA and galanin, actively promotes sleep onset and maintenance by dampening the activity of the ARAS. Conversely, the ARAS, a conglomerate of various brainstem nuclei including the noradrenergic locus coeruleus, serotonergic raphe nuclei, cholinergic pedunculopontine (PPT) and laterodorsal tegmental (LDT) nuclei, and histaminergic tuberomammillary nucleus, diffusely projects to the thalamus and cerebral cortex to establish and sustain arousal and wakefulness (Morris et al., 2012).

The stability and consolidation of these sleep–wake states are critically dependent on the orexin (also known as hypocretin) system, which originates from neurons in the lateral hypothalamus. Orexin neurons exert an excitatory influence on wake-promoting regions, thereby stabilizing wakefulness and preventing inappropriate intrusions of sleep; the pathological loss of these neurons is the primary cause of narcolepsy type 1 (Morris et al., 2012).

The homeostatic drive for sleep (Process S), which intensifies with prolonged wakefulness, is significantly mediated by the neuromodulator adenosine. Adenosine, an endogenous byproduct of cellular energy metabolism, accumulates in the brain during waking hours and is thought to promote sleep by inhibiting wake-active neurons and potentially exciting sleep-promoting VLPO neurons (Morris et al., 2012). Acetylcholine, another key neurotransmitter, exhibits a dual role: it supports cortical arousal and wakefulness when released from basal forebrain and brainstem LDT/PPT neurons, and is also fundamentally involved in an activated state during REM sleep, contributing to its characteristic EEG patterns and atonia (Morris et al., 2012).

Superimposed on these homeostatic and state-dependent mechanisms is the profound influence of the endogenous circadian timing system (Process C), orchestrated by the master biological clock in the suprachiasmatic nucleus (SCN) of the hypothalamus (Morris et al., 2012; Dibner et al., 2010). The SCN projects, often polysynaptically via relay nuclei such as the subparaventricular zone (SPZ) and the dorsomedial hypothalamus (DMH), to key sleep–wake regulatory centers including the VLPO and orexin neurons. Through these pathways, the SCN gates the timing of sleep and wakefulness, aligning them with the 24 h geophysical cycle (Morris et al., 2012).

The primary environmental cue for this daily entrainment is light, perceived by specialized intrinsically photosensitive retinal ganglion cells (ipRGCs) in the retina, which contain the photopigment melanopsin and project directly to the SCN via the retinohypothalamic tract (Berson, 2003). The SCN, in turn, drives robust circadian rhythms in numerous physiological processes that interact with sleep, including the nocturnal synthesis and release of the sleep-permissive hormone melatonin from the pineal gland, and the daily rhythm of cortisol from the adrenal

cortex, which plays an alertness-promoting role, particularly in the morning (Morris et al., 2012).

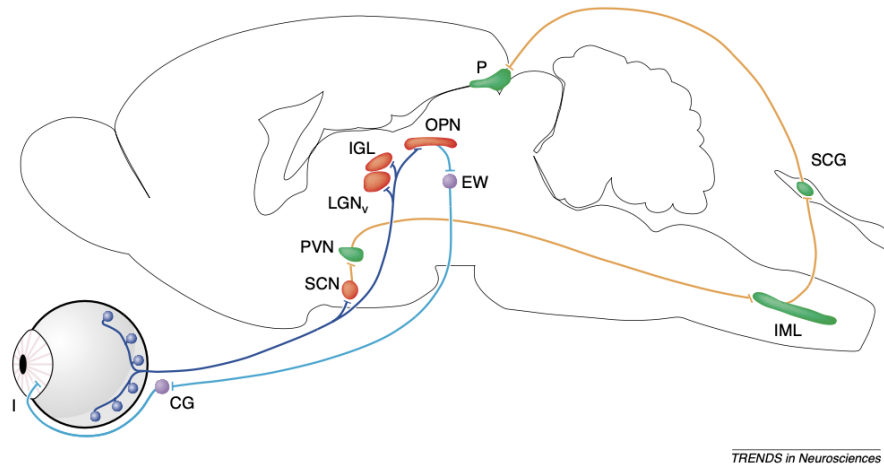


Figure 5: Schematic summary of ipRGC neural pathways. ipRGCs (dark blue) project to primary targets (red), including the SCN for circadian entrainment. The orange pathway with green nuclei shows the SCN-regulated melatonin release circuit via the pineal gland (P), involving the PVN, IML, and SCG. ipRGCs also target the OPN (light blue fibers, purple nuclei), which mediates pupillary light reflexes through the EW, CG, and iris muscles (I). Additional targets include the ventral LGN and IGL of the thalamus.

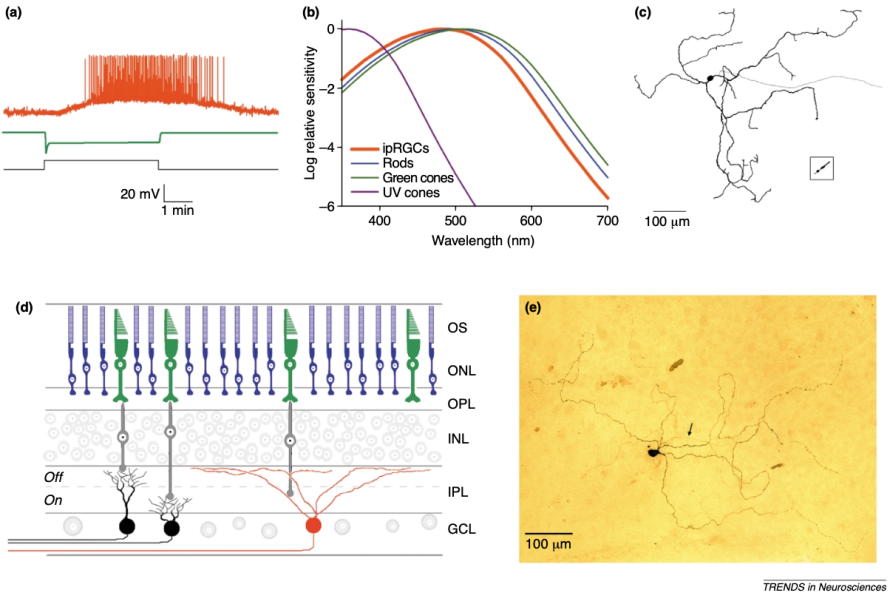


Figure 6: Absorbance spectrum of melanopsin (Berson, 2003)

Neuronal pathways also directly link the SCN to autonomic control centers, such as the paraventricular nucleus of the hypothalamus, influencing cardiovascular parameters through sympathetic and parasympathetic outflows (Morris et al., 2012; Berson, 2003). This complex neurochemical orchestration gives rise to the distinct electrophysiological signatures of wakefulness and each sleep stage, as observed in the electroencephalogram (EEG).

Wakefulness is characterized by high-frequency beta and gamma activity during active cognitive engagement, and alpha rhythms during relaxed states. NREM sleep progresses from stage N1 (theta waves), to N2 (theta waves with sleep spindles and K-complexes—believed to be involved in memory consolidation and sensory gating), and into N3 or slow-wave sleep (SWS), dominated by high-amplitude, low-frequency delta waves considered critical for restorative processes (Driller et al., 2023). REM sleep, despite profound muscle atonia, is characterized by a desynchronized, low-voltage, mixed-frequency EEG pattern that resembles wakefulness, alongside rapid eye movements and vivid dreaming (Driller et al., 2023).

Importantly, these neurophysiological states of sleep and wakefulness are tightly coupled with dynamic changes in autonomic nervous system (ANS) activity. The SCN, through its projections to preautonomic neurons, modulates sympathetic and parasympathetic outflow (Morris et al., 2012; Berson, 2003), leading to characteristic shifts in sympathovagal balance across the NREM–REM cycle, with NREM sleep generally showing parasympathetic dominance and REM sleep exhibiting increased sympathetic lability (Boudreau et al., 2013; Sforza et al., 2016). These

ANS modulations are themselves subject to circadian influence, highlighting the integrated nature of sleep neurophysiology, circadian timing, and autonomic control (Boudreau et al., 2013; Burgess et al., 1997; Trinder et al., 2001; Cosgrave et al., 2021; Natarajan et al., 2025).

2.5 Sleep Regulation: Homeostatic and Circadian Control

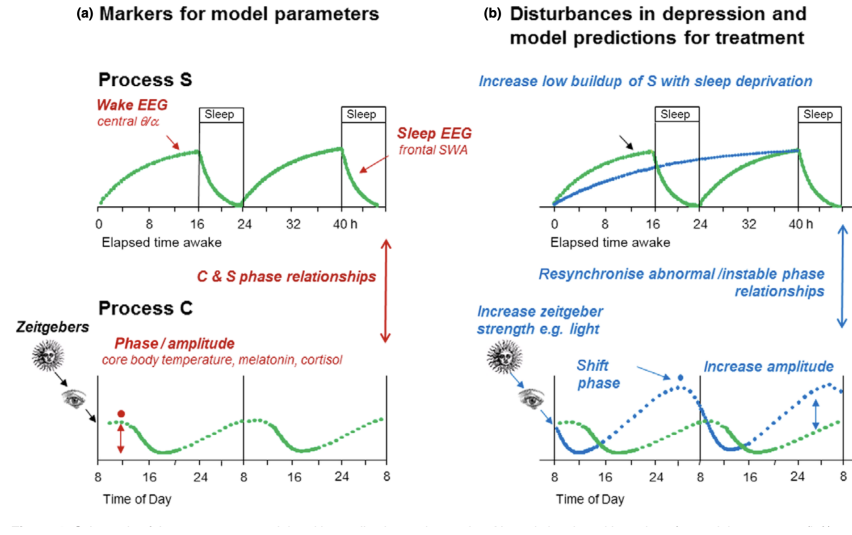


Figure 7: The two-process model of sleep regulation. Process S represents the homeostatic sleep drive that builds during wakefulness and dissipates during sleep. Process C represents the circadian rhythm that modulates alertness independent of prior sleep-wake history. Sleep typically occurs when Process S is high and Process C is low, creating a sleep gate. The interaction of these two processes helps maintain consolidated periods of sleep and wakefulness. Borbély et al., 2016

The timing, duration, and intensity of sleep are primarily governed by the intricate interplay of two fundamental processes: the sleep homeostat (Process S) and the circadian rhythm (Process C), a conceptual framework known as the "two-process model" first proposed and later revised by Borbély et al., 2016. Process S represents the homeostatic drive for sleep, an intrinsic need that accumulates as a function of prior time spent awake and dissipates exponentially during subsequent sleep (Morris et al., 2012). The intensity of slow-wave sleep (SWS), particularly the magnitude of EEG slow-wave activity (SWA; typically defined as power in the 0.5-4.5 Hz range), is widely considered a robust physiological marker of this homeostatic sleep pressure (Morris et al., 2012; Franken and Dijk, 2024). Thus, more extended periods of wakefulness lead to a greater build-up of Process S, resulting in deeper and more

intense SWS. Concurrently, Process C, driven by the endogenous circadian clock located in the suprachiasmatic nucleus (SCN) of the hypothalamus, imposes an approximately 24-hour rhythm on sleep propensity, independent of the duration of prior wakefulness (Morris et al., 2012; Dibner et al., 2010). Process C creates "circadian gates" for sleep and wakefulness, determining times of high and low sleep propensity across the nychthemeron. Under typical conditions, the circadian drive for alertness peaks during the biological day and declines in the evening, promoting sleep onset in conjunction with high homeostatic sleep pressure. Conversely, the circadian alerting signal begins to rise towards the end of the habitual sleep period, facilitating awakening as Process S dissipates (Morris et al., 2012). This interaction ensures consolidated periods of sleep and wakefulness. However, while the two-process model has been immensely influential, recent research, as summarized by Franken and Dijk, 2024, increasingly challenges the notion that Process S and Process C are entirely functionally and mechanistically separate, suggesting a more complex, integrated regulatory system. Evidence indicates that core circadian clock genes can influence markers of sleep homeostasis such as SWA (Morris et al., 2012; Franken and Dijk, 2024). Conversely, perturbations of sleep homeostasis, like sleep deprivation, can alter the rhythmic expression of clock genes in peripheral tissues, and even within the SCN itself under certain conditions (Morris et al., 2012; Franken and Dijk, 2024). Furthermore, the recovery dynamics following sleep loss are multifaceted; while SWA might rebound quickly, the restoration of NREM/REM sleep amounts, sleep architecture, and various molecular and hormonal markers (e.g., cortisol, growth hormone) can follow much slower and more complex time courses. This suggests that sleep homeostasis involves more than the simple dissipation of a single sleep debt indicator manifested by SWA (Morris et al., 2012; Franken and Dijk, 2024). This intricate web of interactions highlights the interdependence of circadian and sleep-wake driven processes at multiple physiological levels, including endocrine and autonomic regulation (Morris et al., 2012; Franken and Dijk, 2024). Therefore, a comprehensive understanding of sleep regulation necessitates considering the dynamic interplay of these processes and their combined impact on a wide range of physiological variables over extended periods, moving beyond a strictly additive model.

2.6 Circadian Rhythms: The Body's Internal Clock

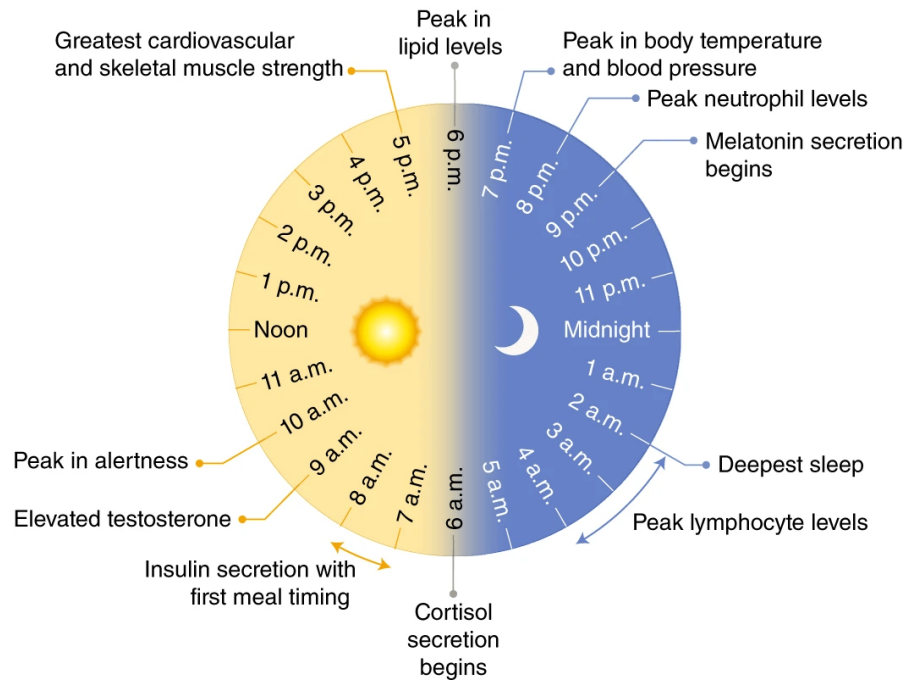


Figure 8: Circadian Rhythm Masri and Sassone-Corsi, 2018

Circadian rhythms are endogenously generated biological rhythms with a period of approximately 24 hours ('circa diem' - about a day) that persist even in the absence of external time cues (Morris et al., 2012; Franken and Dijk, 2024). These rhythms are driven by a master biological clock residing in the suprachiasmatic nucleus (SCN), a small paired structure in the anterior hypothalamus, situated just above the optic chiasm (Morris et al., 2012; Dibner et al., 2010). The SCN functions as an internal pacemaker, allowing organisms to anticipate and adapt to the daily environmental cycles imposed by the Earth's rotation, most notably the light-dark cycle. The SCN exerts its influence through a complex network of neural (e.g., direct and indirect projections to autonomic centers) and humoral (hormonal, such as influencing melatonin release via a polysynaptic pathway involving the paraventricular nucleus and sympathetic ganglia) outputs, thereby orchestrating daily rhythms in a vast array of physiological processes. These include the sleep-wake cycle itself, core body temperature, hormone secretion (particularly **melatonin** and **cortisol**), metabolic functions such as glucose and lipid homeostasis, autonomic nervous system activity, and even cognitive functions like alertness and performance (Morris et al., 2012; Burgess et al., 1997; Gubin et al., 2017; Scheer et al., 2009). While the SCN generates these rhythms endogenously, its intrinsic period is typically slightly

different from exactly 24 hours in humans (on average, about 24.2 hours) (Morris et al., 2012). Therefore, to remain synchronized with the external 24-hour day, the circadian clock must be reset or entrained daily by environmental time cues, known as zeitgebers (from German: *zeit* "time" + *geber* "giver", meaning "time giver" or "synchronizer") (Roenneberg et al., 2003; Phillips et al., 2017). Light is by far the most potent zeitgeber for the SCN (Morris et al., 2012). Light information is transduced by the retina, not only by classical photoreceptors (rods and cones) but critically by a specialized subset of intrinsically photosensitive retinal ganglion cells (ipRGCs). These ipRGCs contain the photopigment melanopsin, which is maximally sensitive to blue-enriched light (around 480nm), and project directly to the SCN core via the retinohypothalamic tract (RHT) (Berson, 2003). The ipRGCs also project to other brain regions mediating non-image forming responses to light, such as the olfactory pretectal nucleus (OPN) for the pupillary light reflex, and indirectly influence melatonin secretion from the pineal gland. The timing, intensity, duration, and spectral composition of light exposure are all critical determinants of its entraining effect, influencing both the phase (timing) and amplitude (strength) of circadian rhythms (Roenneberg et al., 2003; Gubin et al., 2017; Phillips et al., 2017). Other, non-photic zeitgebers, such as the timing of meals, physical activity, social interactions, and even some pharmacological agents, can also exert entraining effects, although their influence is generally weaker than that of light, particularly in humans (Morris et al., 2012). Individuals exhibit natural, and often genetically influenced, variations in their intrinsic circadian timing and sleep-wake preferences, a characteristic known as chronotype (Roenneberg et al., 2003, 2007). Chronotypes range along a continuum from early types ("larks" or M-types), who prefer to wake up and go to bed early and perform optimally in the morning, to late types ("owls" or E-types), who prefer later sleep-wake schedules and peak alertness in the afternoon or evening (Morris et al., 2012). Chronotype can be assessed using validated questionnaires, such as the Horne-Östberg Morningness-Eveningness Questionnaire (MEQ) (Horne and Ostberg, 1976; Gullo et al., 2009), or the Munich ChronoType Questionnaire (MCTQ), which uses self-reported sleep behavior on work-free days (MSF, mid-sleep on free days) as a proxy for an individual's internal circadian time (Roenneberg et al., 2003, 2007). However, especially when assessing individuals with sleep disorders like insomnia, questionnaire-based or sleep-timing-based assessments of chronotype require cautious interpretation, as sleep disturbances can confound these measures (Cosgrave et al., 2021; Tsai et al., 2015; Tackenberg and Hughey, 2021). Physiologically, chronotype is closely linked to the timing of an individual's circadian rhythm of melatonin secretion, specifically the dim light melatonin onset (DLMO), which serves as a robust and widely used marker of internal circadian phase (Phillips et al., 2017). Modern lifestyles, characterized by artificial light exposure at night, irregular work schedules (e.g., shift work), frequent travel

across time zones, and societal pressures for early start times, often lead to a state of circadian misalignment. This occurs when there is a mismatch between the timing of the internal biological clock and the timing of external behavioral and environmental cycles, a phenomenon sometimes quantified as "social jetlag" (Roenneberg et al., 2007; Morris et al., 2012; Phillips et al., 2017; Morris et al., 2016). Such circadian disruption is associated with a wide range of negative health consequences, including impaired sleep quality and quantity, reduced cognitive performance and alertness, and an increased risk for various chronic diseases. These include metabolic disorders (e.g., obesity, type 2 diabetes, metabolic syndrome), cardiovascular diseases (e.g., hypertension), mood disorders (e.g., depression), and potentially an increased risk of certain types of cancer (Morris et al., 2012; Natarajan et al., 2025; Scheer et al., 2009; Morris et al., 2016; Benedetti et al., 2021; Walch et al., 2019). For instance, irregular sleep schedules, which are prevalent in populations such as college students, have been linked to delayed circadian timing (later DLMO), reduced amplitude of daily light exposure rhythms, and poorer academic performance (Phillips et al., 2017). The quantitative analysis of circadian rhythms in physiological and behavioral data often requires specialized time-series analysis methods. These range from simple visualization of raw data and calculation of parameters like acrophase (peak time) and amplitude, to more sophisticated techniques such as cosinor analysis (fitting a cosine wave to the data) or Lomb-Scargle periodograms, the latter being particularly advantageous for detecting rhythmicity in unevenly sampled data, which is common in real-world ambulatory monitoring settings (Cosgrave et al., 2021; Natarajan et al., 2025; Refinetti et al., 2007; Stucky et al., 2021).

2.7 The Autonomic Nervous System (ANS)

The Autonomic Nervous System (ANS) is a critical division of the peripheral nervous system responsible for regulating a wide array of involuntary physiological processes that are essential for maintaining homeostasis and adapting to internal and external demands (Penzel et al., 2003). It exerts control over vital functions such as heart rate, blood pressure, respiration, digestion, glandular secretion, and thermoregulation, operating largely below the level of conscious control. The SCN, the master circadian pacemaker, exerts significant control over the ANS through projections to preautonomic neurons in regions like the paraventricular nucleus (PVN) of the hypothalamus, which in turn modulate sympathetic and parasympathetic outflow (Morris et al., 2012). The ANS comprises two main branches, which often have opposing but functionally complementary actions on target organs (Morris et al., 2012):

- **Sympathetic Nervous System (SNS):** Often characterized as mediating

the "fight-or-flight" response, the SNS prepares the body for action and stress. Activation of the SNS typically leads to an increase in heart rate and contractility, elevation of blood pressure, bronchodilation, mobilization of energy stores (e.g., glucose release), and diversion of blood flow from visceral organs to skeletal muscles (Morris et al., 2012; Penzel et al., 2003).

- **Parasympathetic Nervous System (PNS):** Associated with the "rest-and-digest" or "feed-and-breed" state, the PNS promotes energy conservation, and facilitates restorative and anabolic functions. PNS activation generally results in a decrease in heart rate, a lowering of blood pressure (though less directly than SNS elevates it), bronchoconstriction, and stimulation of digestive processes, including glandular secretions and gut motility (Morris et al., 2012; Penzel et al., 2003).

The dynamic interplay and relative balance between SNS and PNS activity, often referred to as sympathovagal balance, is continuously adjusted to meet the body's physiological needs across different states of wakefulness, physical or mental activity, and sleep (Burgess et al., 1997; Trinder et al., 2001; Penzel et al., 2003). Cardiovascular parameters, particularly heart rate (HR) and its beat-to-beat variability (Heart Rate Variability, HRV), serve as widely utilized and valuable non-invasive proxies for assessing ANS activity and sympathovagal balance (Sforza et al., 2016; Cosgrave et al., 2021; Morris et al., 2016; Penzel et al., 2003). HRV quantifies the fluctuations in the time intervals between consecutive heartbeats (RR intervals) and provides insights into the complex regulatory inputs of both the SNS and PNS branches on the sinoatrial node of the heart. Common HRV metrics, include time-domain measures such as SDNN (standard deviation of all normal-to-normal RR intervals, reflecting overall variability) and RMSSD (root mean square of successive differences between normal heartbeats, primarily reflecting vagal modulation). Frequency-domain measures, derived from spectral analysis of the RR interval time series, are also widely used. These include high-frequency (HF) power (typically 0.15-0.4 Hz), which is a reliable marker of cardiac vagal (PNS) modulation and is closely associated with respiratory sinus arrhythmia (RSA), and low-frequency (LF) power (typically 0.04-0.15 Hz), which is considered to reflect a combination of sympathetic and parasympathetic influences, though its precise interpretation, particularly concerning sympathetic tone, remains a subject of discussion (Sforza et al., 2016; Burgess et al., 1997). The LF/HF ratio has often been used as an index of sympathovagal balance, with higher values suggesting sympathetic predominance and lower values suggesting parasympathetic predominance; however, its interpretation, especially during sleep and under various physiological conditions, requires considerable caution due to the complex interplay of factors influencing LF power (Trinder et al., 2001; Penzel et al., 2003). Other physiological measures, such as

the pre-ejection period (PEP) derived from impedance cardiography, can offer a more specific non-invasive index of cardiac sympathetic activity, though this is less commonly used in ambulatory sleep studies (Burgess et al., 1997; Trinder et al., 2001; Ruf, 1999). Assessing these ANS markers during different physiological states, such as the transition from wakefulness to sleep, across different sleep stages, or in response to orthostatic challenges (e.g., clino-orthostatic tests), provides valuable information about autonomic regulation and its potential alterations in various clinical conditions or under different environmental stressors (Sforza et al., 2016; McDonnell et al., 2021; Rösler et al., 2022). Deviations from normal bedtime routines have also been shown to impact resting heart rate during subsequent sleep and wakefulness, reflecting ANS adjustments (Lunsford-Avery et al., 2018).

2.8 ANS Activity During Sleep

Sleep is accompanied by profound and systematic changes in Autonomic Nervous System (ANS) activity, reflecting a fundamental shift in the body's regulatory priorities from meeting the demands of active wakefulness to facilitating processes of rest, restoration, and energy conservation (Morris et al., 2012; Trinder et al., 2001). Generally, the transition from wakefulness into non-rapid eye movement (NREM) sleep is characterized by a progressive withdrawal of sympathetic nervous system (SNS) tone and a corresponding increase in parasympathetic nervous system (PNS), or vagal, dominance (Sforza et al., 2016; Burgess et al., 1997; Trinder et al., 2001; Snyder et al., 1964). This shift is robustly evidenced by several key physiological changes:

- A gradual decrease in mean heart rate (HR) and blood pressure (BP) as sleep deepens through the NREM stages (Trinder et al., 2001; Cosgrave et al., 2021; Morris et al., 2016; Snyder et al., 1964).
- An increase in HRV metrics predominantly associated with parasympathetic activity. This includes an elevation in the high-frequency (HF) component of the HRV power spectrum (HF power or HFnu when normalized), which reflects respiratory sinus arrhythmia (RSA), a key indicator of vagal cardiac control (Sforza et al., 2016; Burgess et al., 1997; Trinder et al., 2001; Penzel et al., 2003; Whitehurst et al., 2018). Time-domain measures like RMSSD also typically increase (Rösler et al., 2022).
- A corresponding decrease in markers of sympathetic activity. Direct recordings of muscle sympathetic nerve activity (MSNA) show a significant reduction during NREM sleep compared to wakefulness. Indirect markers, such as a lengthening of the pre-ejection period (PEP), also suggest reduced cardiac sympathetic drive (Burgess et al., 1997; Trinder et al., 2001; Ruf, 1999).

This overall shift towards parasympathetic dominance is typically most pronounced during slow-wave sleep (SWS, or N3 sleep), the deepest stage of NREM sleep (Snyder et al., 1964). The heightened vagal tone during SWS is thought to play a crucial role in the restorative functions attributed to this sleep stage, including cardiovascular recuperation, energy conservation, and facilitation of anabolic processes (Whitehurst et al., 2018). Notably, this pattern of increased parasympathetic activity and reduced sympathetic activity during NREM sleep is observed not only during nocturnal sleep periods but also during daytime naps, suggesting a fundamental characteristic of the NREM sleep state itself (Whitehurst et al., 2018). However, studies in Idiopathic Hypersomnia (IH) suggest a persistent rise in HF and HFnu across all NREM stages and REM, coupled with blunted sympathetic indices, indicating a primary PNS dysfunction in these patients (Sforza et al., 2016). In stark contrast, rapid eye movement (REM) sleep exhibits a markedly different and more complex autonomic profile. Despite the characteristic muscle atonia that defines REM sleep, the ANS shows increased lability, with phasic bursts of sympathetic activity superimposed on a background autonomic tone that can sometimes resemble wakefulness or light NREM sleep (Trinder et al., 2001; Morris et al., 2016; Snyder et al., 1964). This results in several distinctive autonomic features during REM sleep:

- An increase in average HR and BP compared to NREM sleep, often approaching or even exceeding waking levels during phasic REM periods (Cosgrave et al., 2021; Morris et al., 2016; Snyder et al., 1964).
- Marked increases in the short-term variability of HR and BP, with significant fluctuations occurring from minute to minute, reflecting the dynamic autonomic shifts (Snyder et al., 1964).
- A shift in the overall sympathovagal balance towards sympathetic predominance or, at least, a significant reduction in parasympathetic influence compared to NREM sleep, as reflected in HRV metrics such as a decrease in HF power and an increase in the LF/HF ratio (Sforza et al., 2016; Trinder et al., 2001; Whitehurst et al., 2018).

These phasic autonomic fluctuations and surges in sympathetic activity during REM sleep, particularly in the REM periods occurring later in the night and into the early morning, have been noted for their potential medical implications, as they may contribute to the increased risk of adverse cardiovascular events observed during these times (Snyder et al., 1964). Furthermore, it is not only the broad sleep stages that modulate ANS activity; transient electrophysiological events within sleep, such as arousals, micro-arousals, K-complexes, and specific phases of the Cyclic Alternating Pattern (CAP), are also associated with brief but

significant modulations of ANS activity, typically involving transient sympathetic surges and heart rate accelerations (Sforza et al., 2016; Cosgrave et al., 2021; Stucky et al., 2021; Penzel et al., 2003; Katori et al., 2022). For instance, Sforza et al., 2016 observed a significantly higher HR arousal response in IH patients compared to controls, persisting into the post-arousal period, suggesting an altered autonomic response. Rösler et al., 2022 found that in individuals with insomnia, HR often increased prior to nocturnal body movements, and this increase was steeper compared to controls, suggesting anticipatory autonomic activation. This intricate coordination between cortical activity (CNS) and cardiac autonomic control (ANS) during sleep underscores the concept of "CNS-ANS coupling," a relationship that is dynamically modulated by sleep architecture, age, and the presence of sleep disorders (Tackenberg and Hughey, 2021; Penzel et al., 2003). Heart rate dynamics during sleep also exhibit different fractal or correlation properties across sleep stages; for example, long-range correlations similar to those seen in wakefulness are observed predominantly during REM sleep, whereas NREM sleep tends to show uncorrelated heart rate patterns beyond the timescale of breathing, suggesting distinct underlying regulatory mechanisms for each sleep state (Bunde et al., 2000). Even the overall contour of the heart rate curve across the entire sleep period, including the timing and depth of its nadir (lowest point), contains valuable information related to sleep structure, circadian timing, and overall health status, independent of simple average or minimum HR values (Natarajan et al., 2025; Fudolig et al., 2024).

2.9 Interaction of Sleep and Circadian Rhythms on ANS

The regulation of Autonomic Nervous System (ANS) activity across the 24-hour day is not solely determined by the prevailing sleep-wake state but is also profoundly influenced by the endogenous circadian system, orchestrated by the suprachiasmatic nucleus (SCN) (Morris et al., 2012). Disentangling the respective contributions of the sleep-wake cycle (a homeostatically driven process) and the circadian rhythm (an endogenously timed process) to ANS function is crucial for a comprehensive understanding of cardiovascular and metabolic regulation. Specialized experimental protocols, such as constant routine (CR) protocols—where individuals are kept awake in a semi-recumbent posture, under dim light conditions, with regular small isocaloric meals, to minimize behavioral and environmental influences—or forced desynchrony protocols—where sleep-wake cycles are scheduled at periods significantly different from 24 hours (e.g., 20-hour or 28-hour "days")—have been instrumental in teasing apart these intertwined influences (Morris et al., 2012; Burgess et al., 1997; Gubin et al., 2017; Ruf, 1999). These studies have revealed that both systems exert significant, and often interactive, control over various ANS parameters. Key findings suggest a differential primary influence on the two main

branches of the ANS:

- **Parasympathetic Activity:** Measures of cardiac parasympathetic modulation, such as respiratory sinus arrhythmia (RSA) or the high-frequency (HF) component of HRV, exhibit a robust endogenous 24-hour rhythm that persists even in the absence of sleep (e.g., during a CR protocol) or when sleep occurs at abnormal circadian phases (during forced desynchrony) (Burgess et al., 1997; Trinder et al., 2001; Ruf, 1999). This indicates a strong and direct influence of the circadian system on vagal tone. For instance, using an ultradian sleep-wake cycle (60 min sleep, 60 min wake), found a significant circadian rhythm of HF power during wakefulness and all NREM sleep stages. They observed that maximal parasympathetic modulation during SWS (characterized by high RRI and HF power) tended to occur around the biological night (approximately 02:00-05:00, relative to the CBT minimum), aligning with the nadir of the core body temperature rhythm, a key marker of circadian phase (Boudreau et al., 2013).
- **Sympathetic Activity:** In contrast, markers of sympathetic activity, such as the pre-ejection period (PEP) or plasma norepinephrine levels, tend to show a clear 24-hour rhythm that is more tightly linked to the occurrence of sleep itself, rather than solely to circadian time (Burgess et al., 1997; Trinder et al., 2001; Ruf, 1999). This suggests that sleep, particularly the transition into and out of sleep, and the REM sleep state, is a dominant driver of the daily rhythm in overall sympathetic tone. Boudreau et al., 2013 reported that during REM sleep, maximal sympathetic modulation (characterized by lower RRI, and a higher LF:HF ratio representing sympathovagal balance) tended to occur in the early morning hours, coinciding with the circadian drive for wakefulness and the peak propensity for REM sleep.

Heart rate (HR) itself is influenced by both systems, demonstrating a clear circadian modulation that is evident even within specific sleep stages (Boudreau et al., 2013; Trinder et al., 2001; Cosgrave et al., 2021; Natarajan et al., 2025). For example, HR during NREM sleep will be lower if that NREM sleep occurs during the biological night compared to the biological day. The interaction between sleep stage and circadian phase is therefore critical. Boudreau et al., 2013 concluded that the circadian and sleep stage-specific effects on HRV are clinically relevant, contributing to the understanding of cardiovascular vulnerability, particularly the morning peak in adverse cardiovascular events. For instance, the steep morning rise in blood pressure and heart rate upon awakening appears to be driven more by the awakening process itself and associated sympathoadrenal activation, rather than by the circadian clock directly, although the circadian system sets the background tone (Morris et al., 2012; Gubin et al., 2017). Understanding this complex interplay

is of significant clinical relevance. Misalignment between the endogenous circadian system and the externally imposed sleep-wake cycle, as commonly experienced by shift workers or individuals with social jetlag, can disrupt these normal ANS patterns, leading to autonomic imbalance, altered cardiovascular reactivity, and contributing to an increased risk for adverse health outcomes such as hypertension, metabolic syndrome, and cardiovascular disease (Scheer et al., 2009; Morris et al., 2016). The traditional two-process model of sleep regulation (Process S - homeostatic, Process C - circadian) provides a foundational framework, but as highlighted by Franken and Dijk, 2024 and supported by such ANS studies, these processes are not entirely independent and interact at multiple physiological levels, including gene expression, hormonal signaling, and direct neural control of autonomic outflow (Morris et al., 2012).

2.10 Factors Influencing Sleep, Circadian Rhythms, and ANS

The intricate regulation of sleep, circadian rhythms, and autonomic nervous system (ANS) function is highly sensitive to a multitude of internal and external factors. These factors can modulate the expression of sleep, shift circadian timing, alter autonomic balance, and ultimately impact overall health and well-being.

- **Light Exposure:** As the primary zeitgeber for the human circadian system, light plays a paramount role (Roenneberg et al., 2003; Morris et al., 2012; Berson, 2003). The timing, intensity, duration, and spectral composition of light exposure significantly influence the phase and amplitude of circadian rhythms, including the sleep-wake cycle and associated hormonal profiles like melatonin (Morris et al., 2012; Gubin et al., 2017; Phillips et al., 2017). Exposure to light, particularly blue-enriched light at inappropriate times, such as in the evening or at night, can acutely suppress melatonin secretion, delay circadian phase (making it harder to fall asleep at a conventional time), and directly impact ANS activity during sleep (Morris et al., 2012; Berson, 2003). For instance, compelling evidence from Mason et al., 2022 demonstrated that even exposure to moderate room light (e.g., 100 lux) during a single night of sleep, compared to sleeping in dim light, was sufficient to increase nighttime heart rate, decrease heart rate variability (specifically, increasing the LF/HF ratio, indicative of a shift towards sympathetic dominance), impair sleep architecture (resulting in less SWS and REM sleep, and more N2 sleep), and notably, increase next-morning insulin resistance. This latter effect was postulated to be mediated, at least in part, by the increased sympathetic nervous system activation during sleep under light exposure conditions (Mason et al., 2022). Conversely, increased daytime light exposure, especially in the morning, can

help advance circadian phase and consolidate nighttime sleep (Roenneberg et al., 2003; Morris et al., 2012). The absence of light during the usual light phase (e.g., prolonged darkness) can also lead to physiological changes, such as a lowering of blood pressure and core body temperature (Gubin et al., 2017). It is also noteworthy that responses of cardiovascular parameters like blood pressure and body temperature to environmental factors such as ambient light may exhibit gender-specific differences, with certain effects being more pronounced in females (Gubin et al., 2017).

- **Sleep Regularity and Timing:** Beyond the total duration of sleep, the consistency or regularity of sleep-wake timing is increasingly recognized as a critical determinant of circadian health and overall well-being (Phillips et al., 2017; Lunsford-Avery et al., 2018). Irregular sleep schedules, which are common in various populations including college students and shift workers, are robustly associated with delayed circadian rhythms (e.g., later dim light melatonin onset - DLMO), altered patterns of daily light exposure (often reduced daytime and increased nighttime light), and negative functional outcomes such as poorer academic or work performance (Phillips et al., 2017; Tsai et al., 2015). Lunsford-Avery et al., 2018 provided striking evidence that even relatively small deviations in bedtime can impact cardiovascular function; their study using Fitbit Charge HRs found that going to bed just 30 minutes later than an individual's usual bedtime was associated with a significant elevation in resting heart rate during the subsequent sleep period and extending into the following day. This highlights the acute sensitivity of the cardiovascular system to bedtime variability. On a broader scale, greater day-to-day variability in sleep timing, often quantified by metrics such as the Sleep Regularity Index (SRI), has been linked to an increased prevalence of cardiometabolic risk factors. For example, lower SRI values (indicating more irregular sleep) in older adults were associated with higher rates of obesity, hypertension, dyslipidemia, hyperglycemia, and a consequently higher 10-year cardiovascular disease risk, even after adjusting for average sleep duration (Phillips et al., 2017; Morris et al., 2016; Walch et al., 2019).
- **Sleep Disorders:** The presence of underlying sleep disorders intrinsically involves disruptions to normal sleep patterns and often has profound impacts on both circadian rhythmicity and autonomic function (Sateia, 2014). The International Classification of Sleep Disorders, Third Edition (ICSD-3), provides the standard nosological framework for these conditions (Sateia, 2014).
 - *Insomnia:* Chronic insomnia is frequently conceptualized as a disorder of 24-hour hyperarousal, involving cognitive, emotional, and physiological

overactivation (Morin et al., 2015). This physiological hyperarousal often manifests as altered ANS activity both during wakefulness and sleep. Studies have reported higher mean heart rate, reduced overall HRV (e.g., lower SDNN), particularly in insomnia patients with objectively short sleep duration, a blunted reduction in heart rate from wakefulness to sleep (indicating impaired parasympathetic engagement at sleep onset), and potentially altered heart rate responses preceding movements during sleep (Cosgrave et al., 2021; Tsai et al., 2015; Tackenberg and Hughey, 2021; Stucky et al., 2021; Rösler et al., 2022). Cosgrave et al., 2021 found that young poor sleepers had significantly higher mean HR in all sleep stages (except N1) and a lower wake-sleep HR reduction compared to good sleepers. When restricted to insomnia with objectively short sleep duration, lower SDNN was observed. Rösler et al., 2022 noted an attenuated cardiac response to sleep in insomnia, with smaller day-night differences in HR and HRV, and that HR increased more steeply prior to nocturnal body movements in insomnia. These persistent autonomic alterations are thought to contribute to the well-documented increased cardiovascular risk observed in individuals with chronic insomnia (Tackenberg and Hughey, 2021; Morris et al., 2016).

- *Central Disorders of Hypersomnolence:* In contrast to the hyperarousal seen in insomnia, some central disorders of hypersomnolence may involve distinct patterns of ANS dysregulation. For instance, Sforza et al., 2016 found that patients with Idiopathic Hypersomnia (IH) exhibited increased markers of parasympathetic activity (HF and HFnu) during both wakefulness and across all sleep stages (light, SWS, and REM), associated with blunted sympathetic indices, compared to controls. Furthermore, IH patients showed a significantly higher HR arousal response that persisted longer into the post-arousal period. These findings suggest an impaired parasympathetic function or a primary dysfunction of parasympathetic activity in IH, rather than sympathetic hyperarousal (Sforza et al., 2016). Narcolepsy, particularly Narcolepsy Type 1 (associated with orexin deficiency), has also been associated with various forms of ANS dysfunction, often implicating alterations in sympathetic pathways, although findings can be complex and varied (Morris et al., 2012).
- *Sleep-Related Breathing Disorders:* Obstructive Sleep Apnea (OSA) is a highly prevalent disorder characterized by recurrent episodes of partial or complete upper airway collapse during sleep, leading to intermittent hypoxia, hypercapnia, sleep fragmentation due to frequent arousals, and significant intrathoracic pressure swings. These cyclical physiological

insults result in sustained sympathetic overactivity, both during sleep and extending into wakefulness, contributing to nocturnal and daytime hypertension, endothelial dysfunction, inflammation, and a substantially elevated risk for a wide range of cardiovascular diseases, including stroke, myocardial infarction, and atrial fibrillation (Morris et al., 2016; Penzel et al., 2003).

- *Circadian Rhythm Sleep-Wake Disorders (CRSWD)*: These disorders stem from a misalignment between an individual's endogenous circadian rhythm and their desired or environmentally/socially imposed sleep-wake schedule (e.g., Delayed Sleep-Wake Phase Disorder, Advanced Sleep-Wake Phase Disorder, Shift Work Disorder), or from a failure of the circadian pacemaker itself (e.g., Irregular Sleep-Wake Rhythm Disorder) (Morris et al., 2012; Sateia, 2014). The resultant chronic circadian disruption not only impairs sleep timing and quality but also leads to desynchronization of peripheral organ clocks, contributing to adverse metabolic (e.g., increased risk of diabetes, obesity) and cardiovascular consequences (e.g., hypertension) (Scheer et al., 2009; Morris et al., 2016).
- **Age and Sex:** Chronotype exhibits significant variation with age, with a well-documented tendency towards later chronotypes (eveningness) during adolescence and young adulthood, followed by a gradual shift towards earlier chronotypes (morningness) with advancing age (Roenneberg et al., 2007; Morris et al., 2012). Sex differences in chronotype are generally small, though some studies suggest males may be, on average, slightly later types than females (Roenneberg et al., 2007; Natarajan et al., 2025). Hormonal fluctuations related to the menstrual cycle in females can also influence sleep architecture and circadian rhythms (Morris et al., 2012).
- **Other Factors:** A host of other behavioral and physiological factors can acutely or chronically influence sleep, circadian rhythms, and ANS activity. These include physical activity (timing and intensity can modulate sleep and circadian phase), meal timing (which can act as a zeitgeber for peripheral clocks), posture (which influences ANS balance), psychological stress (a potent activator of the SNS and HPA axis), and caffeine or alcohol consumption (Morris et al., 2012; Natarajan et al., 2025; McDonnell et al., 2021). Hormonal fluctuations across the day, governed by both sleep-dependent release and the circadian system (e.g., growth hormone, prolactin, TSH), also interact with and influence ANS regulation (Morris et al., 2012). Furthermore, an individual's overall psychological well-being and affective state have been shown to correlate with specific patterns of ANS reactivity and baseline tone (McDonnell et al., 2021; Rösler et al., 2022).

2.11 Measuring Sleep and ANS Activity: From PSG to Wearables

The assessment of sleep, circadian rhythms, and associated physiological changes, including autonomic nervous system (ANS) activity, has traditionally relied on laboratory-based techniques, with polysomnography (PSG) serving as the undisputed gold standard for sleep evaluation (Morris et al., 2012; Sateia, 2014). PSG involves the simultaneous recording of multiple physiological signals, including electroencephalography (EEG) for brain activity, electrooculography (EOG) for eye movements, electromyography (EMG) for muscle tone, electrocardiography (ECG) for cardiac activity, as well as measures of respiratory effort and airflow, oxygen saturation, and limb movements. This comprehensive approach allows for detailed sleep staging, the identification of sleep-disordered breathing events, and the assessment of cardiac function during sleep (Sforza et al., 2016; Cosgrave et al., 2021). However, PSG is expensive, labor-intensive, requires a specialized laboratory setting and trained technicians, and its inherently obtrusive nature can disrupt natural sleep patterns. These limitations restrict its feasibility for long-term, large-scale, or ecologically-valid ambulatory monitoring (Morris et al., 2016; Rösler et al., 2022; Schlagintweit et al., 2023). Ambulatory PSG, as used by Cosgrave et al., 2021 and Sforza et al., 2016 in home environments, mitigates some of the lab-based artificiality but still involves a complex setup. Wrist actigraphy, which uses small, wrist-worn accelerometer-based devices to measure movement, offers a less invasive and more cost-effective alternative for estimating sleep-wake patterns (e.g., total sleep time, sleep efficiency, wake after sleep onset, sleep latency) over extended periods in an individual's natural environment (Suh et al., 2017; Morris et al., 2012; Rösler et al., 2022). While valuable for longitudinal assessment of sleep duration and timing, and for inferring circadian activity rhythms (Natarajan et al., 2025), standard actigraphy provides no direct information on sleep stages or detailed autonomic function (Morris et al., 2012). Subjective measures, such as sleep diaries and standardized questionnaires (e.g., the Pittsburgh Sleep Quality Index - PSQI (Buysse et al., 1989), Epworth Sleepiness Scale - ESS (Johns, 1991), Horne-Östberg Morningness-Eveningness Questionnaire - MEQ (Horne and Ostberg, 1976), and Munich ChronoType Questionnaire - MCTQ (Roenneberg et al., 2003)), provide important contextual information on perceived sleep quality, daytime sleepiness, and chronotype. However, these measures are susceptible to recall bias, subjective interpretation, and may not always align perfectly with objective physiological measures (Morris et al., 2012; Cosgrave et al., 2021). The recent and rapid proliferation of consumer-grade wearable devices (e.g., smart-watches, fitness trackers, rings) equipped with a variety of sensors, most commonly accelerometers for motion tracking and photoplethysmography (PPG) for heart rate monitoring, has opened unprecedented new avenues for unobtrusive, continuous,

and longitudinal monitoring of sleep, activity, and various physiological parameters in real-world, free-living conditions (Natarajan et al., 2025; Morris et al., 2016; Walch et al., 2019; Lunsford-Avery et al., 2018; Katori et al., 2022; Fudolig et al., 2024; Mason et al., 2022; Lee et al., 2024; de Zambotti et al., 2016). These devices hold immense potential for large-scale epidemiological research, personalized health interventions, and clinical applications, particularly in understanding the complex interplay of sleep, circadian rhythms, and autonomic function in daily life. For instance, Lunsford-Avery et al., 2018 utilized data from Fitbit Charge HRs to demonstrate how even minor deviations from usual bedtime affect resting heart rate during sleep. Similarly, Natarajan et al., 2025 leveraged large-scale heart rate and activity data from wrist-worn wearables to model and characterize circadian rhythms, showing, for example, that in most individuals, the circadian rhythm of heart rate lags that of activity. Rösler et al., 2022 used ambulatory ECG and actigraphy to study micro-scale cardiac changes around movements in insomnia. Validation studies comparing the performance of these consumer wearable devices against the gold standard PSG have yielded mixed but increasingly promising results, particularly for certain parameters:

- **Sleep/Wake Detection:** Most modern wearables generally show high sensitivity in correctly identifying periods of sleep but tend to have lower specificity in correctly identifying periods of wakefulness, often leading to an overestimation of total sleep time (TST) and an underestimation of wake after sleep onset (WASO) when compared to PSG (Suh et al., 2017; Morris et al., 2016; Schlagintweit et al., 2023; de Zambotti et al., 2016). de Zambotti et al., 2016 found the Fitbit ChargeHR had high overall accuracy (91%) and sensitivity (97%) for sleep but poor specificity (42%) for wake in adolescents. However, their accuracy for overall sleep-wake discrimination can rival that of research-grade actigraphy devices (Suh et al., 2017).
- **Heart Rate Monitoring:** PPG-derived heart rate (HR) from many wearables generally demonstrates good correlation and relatively small mean bias when compared to ECG-derived HR during sleep, particularly at lower heart rates characteristic of sleep (Natarajan et al., 2025; Benedetti et al., 2021; Schlagintweit et al., 2023; de Zambotti et al., 2016). de Zambotti et al., 2016 reported that the Fitbit ChargeHR underestimated ECG HR by a negligible 0.88 bpm during sleep epochs. Accuracy may decrease during periods of significant movement, during wakefulness, or at higher heart rates (Benedetti et al., 2021; Schlagintweit et al., 2023). Some studies have noted state-specific biases, such as a larger underestimation of HR by PPG during wakefulness or N1 sleep compared to deeper NREM stages (Schlagintweit et al., 2023). The extraction of reliable beat-to-beat intervals for detailed HRV analysis from PPG can be

more challenging than from ECG, but progress is being made.

- **Sleep Staging:** Many consumer wearables now provide proprietary algorithms for estimating sleep stages (typically categorized as Light Sleep, Deep Sleep (SWS), and REM Sleep). Validation results against PSG for sleep staging have been highly variable across devices and algorithms. Some studies show reasonable agreement for certain stages (e.g., REM detection can be fair, and SWS detection is improving), but generally poorer performance for accurately distinguishing between light sleep stages (N1 and N2) or quantifying stage N1 (Suh et al., 2017; Morris et al., 2016; Schlagintweit et al., 2023; de Zambotti et al., 2016). Performance can often be improved by utilizing advanced machine learning models trained on raw sensor data (e.g., multi-axis acceleration and PPG signals) and incorporating additional features such as circadian clock proxies (time of day) or features derived from topological data analysis (Suh et al., 2017; Walch et al., 2019; Katori et al., 2022; Lee et al., 2024; Faust et al., 2020).
- **Novel Metrics and Circadian Assessment:** The rich, longitudinal data streams from wearables enable the exploration and derivation of novel metrics that go beyond traditional sleep summary statistics. These include analyzing the shape characteristics of the sleeping heart rate curve (e.g., timing of the nadir) (Fudolig et al., 2024), deriving circadian parameters (e.g., acrophase, amplitude, period) from continuous HR and activity data using methods like cosinor analysis or Fourier analysis (Suh et al., 2017; Natarajan et al., 2025), or applying advanced signal processing techniques such as Derivative Segment Approximation (DSA) to identify patterns correlated with sleep-wake states or arousals (Lee et al., 2024; Faust et al., 2020). Combining cardiac monitoring with actigraphy, as done by Rösler et al., 2022, may aid in the objective quantification of conditions like insomnia by assessing state-related cardiac changes.

Despite their transformative potential, the use of consumer wearables in research and clinical settings is not without limitations. These include the often proprietary ("black box") nature of the data processing algorithms, a lack of direct access to raw sensor data for many devices (hindering independent validation and development of custom algorithms), variability in sensor quality and data accuracy across different devices and wearing conditions, and the ongoing need for rigorous, independent validation studies across diverse populations and clinical conditions (Suh et al., 2017; Walch et al., 2019; Schlagintweit et al., 2023; Lee et al., 2024; de Zambotti et al., 2016). Notwithstanding these challenges, the ability to collect vast amounts of rich, longitudinal physiological and behavioral data in naturalistic, free-living settings makes wearables exceptionally powerful tools for advancing our understanding of

the complex and dynamic interplay of sleep, circadian rhythms, and autonomic function in human health and disease.

2.12 Sleep indices

Sleep indices are quantitative measures used to assess various aspects of sleep quality and quantity. These metrics help in diagnosing sleep disorders and evaluating treatment effectiveness.

2.12.1 Sleep Duration (SD)

Amount of time elapsed between sleep onset and sleep offset.

$$SD = S_{\text{offset}} - S_{\text{onset}} \quad (9)$$

2.12.2 Wake After Sleep Onset (WASO)

WASO quantifies the total time spent awake after initially falling asleep:

$$\text{WASO} = \text{Total Duration of Wake Episodes (in minutes)} \quad (10)$$

2.12.3 Total Sleep Time (TST)

Total Sleep Time measures the actual time spent asleep during the sleep period:

$$\text{TST} = SD - \text{WASO} \quad (11)$$

2.12.4 Sleep Efficiency (SE)

Sleep efficiency is the percentage of time spent asleep during a period of sleep.

$$SE = \frac{\text{TST}}{SD} \times 100\% \quad (12)$$

2.12.5 Sleep Onset Latency (SOL)

Sleep Onset Latency measures the time taken to fall asleep after going to bed:

$$\text{SOL} = t_{\text{sleep_onset}} - t_{\text{lights_off}} \quad (13)$$

2.12.6 Sleep Stage Distribution (SSD)

SSD calculates the percentage of time spent in each sleep stage:

$$\text{SSD}_{\text{stage}} = \frac{\text{Time in Stage}}{\text{TST}} \times 100\% \quad (14)$$

2.12.7 Sleep Regularity Index (SRI)

The Sleep Regularity Index (SRI) is a measure that assesses the probability that an individual is awake (vs. asleep) at any two time points 24 h apart (Phillips et al., 2017 Lunsford-Avery et al., 2018).

The formula used for SRI is as follows:

$$SRI = -100 + \frac{200}{M(N-1)} \sum_{j=1}^M \sum_{i=1}^{N-1} \delta(s_{i,j}, s_{i+1,j}) \quad (15)$$

where N is the number of days of recording, M is the number of epochs per day, $s_{i,j}$ is the sleep state at time epoch j of day i , and δ is the Kronecker delta function that returns 1 if $s_{i,j} = s_{i+1,j}$ and 0 otherwise.

For example, consider a 2-dimensional matrix representing sleep states over 3 days, with each day divided into 4 time epochs:

$$S = \begin{bmatrix} 1 & 1 & 0 & 0 \\ 1 & 1 & 0 & 0 \\ 0 & 1 & 1 & 0 \end{bmatrix}$$

where each row represents a day, each column represents a time epoch, and the values indicate sleep state (1 = asleep, 0 = awake).

The SRI would be computed:

$$SRI = -100 + \frac{200}{4(2)} \sum_{j=1}^4 \sum_{i=1}^2 \delta(s_{i,j}, s_{i+1,j}) \quad (16)$$

$$= -100 + \frac{200}{8} \cdot (4 + 2) \quad (17)$$

$$= -100 + \frac{200}{8} \cdot 6 \quad (18)$$

$$= -100 + 150 = 50 \quad (19)$$

2.12.8 Mid Sleep Point (MSP)

The Mid Sleep Point (MSP), as described by Terman et al., 2001, is the midpoint of the sleep period:

$$MSP = S_{\text{onset}} + \frac{S_{\text{offset}} - S_{\text{onset}}}{2} \quad (20)$$

Where S_{onset} is the datetime representation of the sleep onset time, and S_{offset} is the datetime representation of the sleep offset time.

In absence of a datetime object representation of data, MSP can be calculated as a midpoint between two circular coordinates with the following approach:

$$\begin{aligned}
 \theta_i &= \frac{\text{minutes since midnight}_i}{1440} \times 2\pi && \text{Convert times to angles} \\
 x_i &= \cos(\theta_i), \quad y_i = \sin(\theta_i) && \text{Convert to Cartesian coordinates} \\
 x_{\text{mid}} &= \frac{x_1 + x_2}{2}, \quad y_{\text{mid}} = \frac{y_1 + y_2}{2} && \text{Find midpoint} \\
 \theta_{\text{mid}} &= \text{atan2}(y_{\text{mid}}, x_{\text{mid}}) && \text{Convert back to angle} \\
 \text{MSP (minutes)} &= \frac{\theta_{\text{mid}}}{2\pi} \times 1440 && \text{Convert to minutes} \tag{21}
 \end{aligned}$$

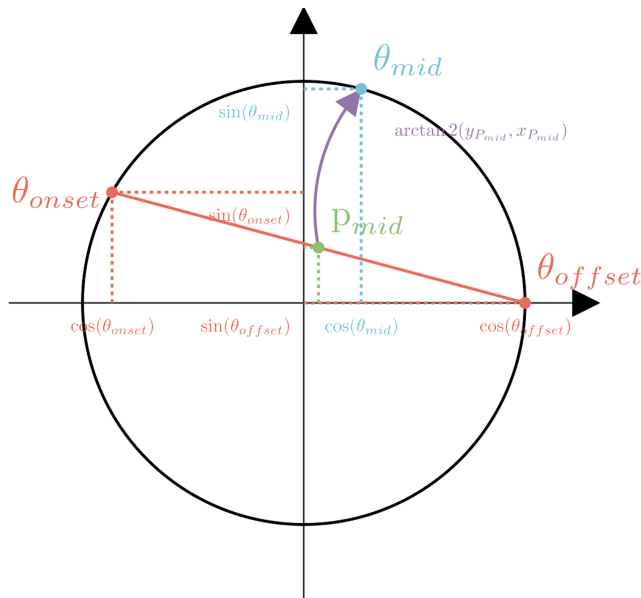


Figure 9: Visual representation of Mid Sleep Point (MSP) calculation showing the midpoint between sleep onset and offset times

2.12.9 Number of Awakenings (NAw)

Number of distinct awakenings during the sleep period.

2.12.10 Activity Index (ActI)

Absolute duration (in minutes) where the activity vector has a value not equal to zero.

2.12.11 Movement Index (MovI)

Relative percentage of time in which there was activity (non-zero values in activity vector) compared to the total duration of the sleep episode.

2.12.12 Fragmentation Index (FI)

The Fragmentation index is the number of awakenings per hour of sleep.

$$FI = \frac{NAw}{SD/h} \quad (22)$$

2.12.13 Sleep Fragmentation Index (SFI)

The Sleep Fragmentation Index is the sum of the Movement Index and the Fragmentation Index. It is particularly useful for assessing the quality of sleep and risk of OSAS.

$$SFI = FI + MI \quad (23)$$

2.12.14 Apnea Hypopnea Index (AHI)

The Apnea Hypopnea Index is the number of apneas and hypopneas per hour of sleep.

$$AHI = \frac{\text{Total Apneas and Hypopneas Eps.}}{SD/h} \quad (24)$$

2.13 Chronobiometrical Analysis of Sleep

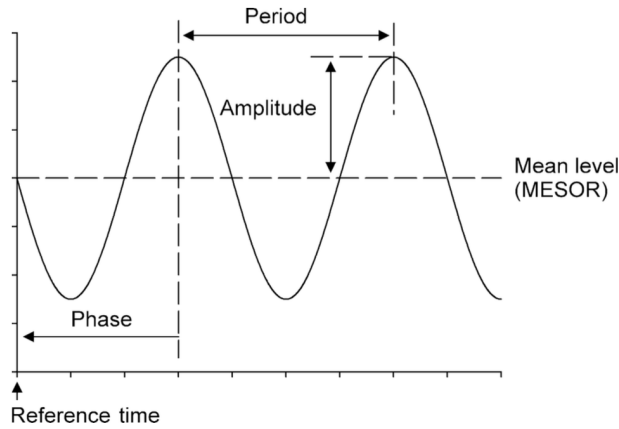


Figure 10: Visual representation of the oscillatory process of a signal Refinetti et al., 2007

The analysis of oscillatory signals in chronobiology involves several key parameters that characterize the rhythmic patterns:

2.13.1 Period

The period (τ) is the time required to complete one full cycle of oscillation, measured from peak to peak or trough to trough. For circadian rhythms, this is approximately 24 hours.

2.13.2 Mesor

The Midline Estimating Statistic Of Rhythm (MESOR) represents the rhythm-adjusted mean, calculated as the average value around which the oscillation occurs. For a time series $x(t)$, the MESOR (M) can be expressed as:

$$M = \frac{1}{T} \int_0^T x(t) dt \quad (25)$$

where T is the total time period of observation.

2.13.3 Amplitude

The amplitude (A) is half the difference between the peak and trough values of the rhythm. It quantifies the extent of rhythmic change:

$$A = \frac{x_{\max} - x_{\min}}{2} \quad (26)$$

2.13.4 Acrophase

The acrophase (ϕ) represents the time at which the peak of the rhythm occurs, usually expressed in degrees or radians relative to a reference time (often midnight or dawn). For a signal with period τ , the acrophase can be calculated as:

$$\phi = 2\pi \frac{t_{\text{peak}}}{\tau} \quad (27)$$

where t_{peak} is the time of peak occurrence.

2.13.5 Phase

The phase describes the timing of any point in the rhythm relative to a reference point. While acrophase specifically refers to the timing of the peak, phase can refer to any characteristic point in the cycle. The phase angle (θ) between two rhythms can be calculated as:

$$\theta = 2\pi \frac{\Delta t}{\tau} \quad (28)$$

where Δt is the time difference between corresponding points in the two rhythms.

These parameters can be estimated using various mathematical methods, including cosinor analysis, which fits a cosine function to the data:

$$x(t) = M + A \cos \left(\frac{2\pi t}{\tau} + \phi \right) + \epsilon(t) \quad (29)$$

where $\epsilon(t)$ represents the error term.

3 Materials

3.1 Software Environment

Software	Version	Purpose
Python	3.11.x	Primary programming language
Pandas	2.2.0	Data manipulation and analysis
Numpy	2.2.2	Numerical computing
SciPy	1.12.0	Scientific computing
Scikit-learn	1.4.x	Machine learning toolkit
Statsmodels	0.14.0	Statistical modeling and testing
PyMC3	4.11.5	Bayesian modeling and inference
Umap	0.1.1	Dimensionality reduction
ephem	4.14.0	Library for high-precision astronomy computations
Matplotlib	3.8.2	Data visualization
Seaborn	0.13.0	Data visualization

Table 1: Software Stack Specifications

3.2 Data Collection

Demographic data along with the sleep data has been collected and provided by the Sleepacta platform.

The following inclusion criteria were applied to the data to ensure that only relevant records were included in the analysis:

1. Population of healthy adults aged 18-75 years
2. Fitbit provided of an HR sensor (PhotoPlethysmography) was used to collect the data
3. Exams must not contain relevant artifacts during night-time that could affect the sleep detection algorithm
4. Contain exams with at least 3 main night sleep episodes
5. Exams must contain all demographic data (age, gender, weight, height)

4 Methods

4.1 Experimental Protocol

The experimental procedure, implemented within the sleep analysis Python package, follows these steps:

Overall Aim

The pipeline aims to identify distinct sleep phenotypes based primarily on heart rate characteristics during sleep episodes. By transforming raw heart rate time series into meaningful features, we aim to:

- Identify sleep phenotypes by clustering episodes with similar heart rate dynamics and nadir timing patterns using KMeans. The optimal number of clusters (k) is determined via Silhouette analysis on either nadir timing or UMAP-reduced heart rate features.
- Examine the relationship between these phenotypes and both sleep-related and demographic factors through comprehensive statistical modeling.
- Investigate potential causal pathways between subject characteristics and phenotype membership by adjusting for confounders identified through a Directed Acyclic Graph (DAG) approach.

4.1.1 Preprocessing

The pipeline starts by loading raw data from tabular data files, each row representing a single sleep episode. Preprocessing functions (e.g., for HR cleaning) are applied to the heart rate (HR) time series of each episode. Subject-level characteristics (age, sex, BMI, etc.) and general sleep indices (e.g., `tst` mean, `SRI`) are retained. The HR time series are standardized in length using a dedicated function (e.g., `equalize_hr`), which employs Piecewise Aggregate Approximation (PAA) to achieve a fixed `TARGET_LEN` (e.g., 100 points).

4.1.2 Feature Extraction Pipeline Step

Each episode's cleaned and length-equalized heart rate series is processed to generate engineered features. A key feature is the Topological Data Analysis (TDA) vector (`tda_vector`), a 2-dimensional summary derived from the HR first derivative (`slope_fixed_len`). This involves creating a time-delay embedding of the slope with a specific `window_size` (30), computing its persistence diagram using Vietoris-Rips persistence (`VietorisRipsPersistence`), and then calculating the persistence

entropy (`PersistenceEntropy`). This captures structural patterns in the HR dynamics. Nadir timing features are extracted using a dedicated feature extraction function. This function identifies the time and value of the minimum HR during sleep, considering either actual timestamped HR data (`hr_times`, `hr_values`) if available, or using the length-equalized HR (`hr_eq`) otherwise. Key features include `nadir_time_pct` (percentage into the sleep period), `nadir_time_hours`, `nadir_hr`, and `time_to_nadir_normalized`. A user-defined weight (`nadir_weight`) controls the influence of the normalized nadir time feature in subsequent steps. Subject chronotype is calculated by a dedicated function, yielding per-episode deviations (e.g., `chronotype_desync`, `abs_chronotype_desync`) from the subject average.

Table 2: Variable Groups, Abbreviations, and Descriptions

Group	Variable (x)	Description
Demographical Variables		
	Age	Participant's age in years
	Sex	Participant's sex (F/M)
	BMI	Body Mass Index: $\frac{\text{Weight (kg)}}{\text{Height (m)}^2}$
Sleep Variables (Subject Level)		
	SRI	Sleep Regularity Index
	Chronotype	Subject's average midsleep time (hours from 18:00)
	MSP	Subject's average midsleep point
Sleep Variables (Episode Level)		
	Duration	Sleep episode duration (seconds)
	SE	Sleep Efficiency (TST/WASO %)
	WASO	Wake After Sleep Onset (minutes)
	SFI	Sleep Fragmentation Index
	Activity Index	Index of activity during sleep
	Chronotype Desync	Episode midsleep deviation from subject average (hours)
	Abs Chronotype Desync	Absolute episode midsleep deviation (hours)
Heart Rate Features (Episode Level)		
	RHR	Mean Heart Rate during sleep episode (bpm)
	HR _{Nadir}	Minimum Heart Rate during sleep episode (bpm)
	Nadir Time Pct	Time of HR nadir (% of sleep duration)
	HR Vector	Heart rate time series (sampling 1 per minute)
Derived Features		
	Topological Features	Persistence entropy vector from HR slope
	Cluster Label	Assigned sleep pattern cluster ID
	Cluster Consistency	Subject's consistency metric (1 - normalized entropy)
	Modal Proportion	Proportion of episodes in subject's modal cluster

4.1.3 Dimensionality Reduction and Clustering

- The feature matrix is constructed from two primary components: (1) Topological Data Analysis (TDA) vectors derived from heart rate dynamics, and (2) normalized nadir timing information when available.
- The base feature matrix \mathbf{X} is created by stacking the 2-dimensional TDA vectors from each sleep episode, capturing the essential topological characteristics of heart rate derivative patterns during sleep.

- For nadir timing processing, the pipeline:
 - Identifies and imputes missing values in the raw `nadir_time_pct` values with the median
 - Normalizes the values to a [0,1] range to standardize their scale
- The resulting normalized and weighted nadir timing values are then column-stacked with the TDA vectors to form the combined feature matrix `X_combined`.
- This multi-component representation effectively captures both the morphological dynamics of heart rate changes (through TDA vectors) and the timing of the physiologically significant HR minimum (through nadir timing), providing a more comprehensive characterization of sleep patterns.

This combined matrix undergoes dimensionality reduction using Uniform Manifold Approximation and Projection (UMAP) to generate a 2-dimensional embedding. This non-linear dimensionality reduction technique preserves both local and global topological structures of the high-dimensional data, making it well-suited for visualizing and clustering complex physiological patterns. The UMAP transformation employs parameters such as `n_neighbors` (dynamically calculated based on sample size), `min_dist=0.1`, `metric="euclidean"`, and a fixed random state for reproducibility.

The UMAP-based KMeans clustering strategy with optimal k selection proceeds as follows:

- First, to determine the optimal number of clusters (k), an iterative process is undertaken: for each candidate value of k within a specified range (from `min_clusters` to `max_clusters`), KMeans clustering is performed on the 2D UMAP embedding. The resulting cluster formations are then evaluated using standard metrics, including the Silhouette score and the Calinski-Harabasz index, to gauge clustering quality. The Silhouette score measures how similar points are to their own cluster compared to other clusters, while the Calinski-Harabasz index evaluates cluster separation using the ratio of between-cluster variance to within-cluster variance.
- The optimal k is chosen based on an adjusted Silhouette score.
- Once the optimal k is determined, a KMeans clustering model is configured with this value and fitted directly to the same 2D UMAP embedding that was used for optimal k selection. This final clustering step yields the definitive cluster labels assigned to each sleep episode.

This process, which leverages the UMAP embedding for both the determination of the optimal k and the final clustering assignment, produces the episode cluster labels. The approach capitalizes on UMAP's ability to preserve meaningful relationships in the data while reducing dimensionality, followed by an objective determination of the optimal cluster count and robust KMeans clustering. Alternative strategies such as meta-clustering or different primary clustering algorithms like DBSCAN did not yield easily interpretable results for cluster characterization.

4.1.4 Subject-Level Cluster Consistency and Analysis

After episodes are clustered, results are aggregated at the subject level to analyze pattern stability. Two key metrics are calculated to quantify how consistently a subject's sleep episodes are assigned to the same cluster:

- *Modal proportion*: The proportion of a subject's episodes falling into their most frequent (modal) cluster. This is calculated as:

$$\text{modal_proportion} = \frac{n_{\text{modal}}}{n_{\text{total}}} \quad (30)$$

where n_{modal} is the count of episodes in the most frequent cluster and n_{total} is the total number of episodes for that subject.

- *Entropy-based consistency score*: This utilizes information theory to provide a more nuanced measure that accounts for the full distribution across clusters:

$$\text{consistency} = 1 - \frac{H(X)}{H_{\max}} \quad (31)$$

where $H(X)$ is the Shannon entropy of the cluster distribution and H_{\max} is the maximum possible entropy.

The Shannon entropy is calculated as:

$$H(X) = - \sum_{i=1}^k p_i \log_2 p_i \quad (32)$$

where p_i is the proportion of episodes in cluster i , and k is the number of different clusters observed for that subject.

The maximum entropy is:

$$H_{\max} = \log_2(\min(k, n_{\text{total}})) \quad (33)$$

which represents the entropy if episodes were uniformly distributed across all possible clusters (limited by either the number of available clusters or the number of episodes).

- The entropy-based consistency score ranges from 0 (complete inconsistency, with episodes evenly distributed across clusters) to 1 (perfect consistency, with all episodes in a single cluster).
- Other subject characteristics are aggregated (e.g., mean sleep efficiency, mean wake after sleep onset, age, sleep regularity index) to enable statistical analyses.
- Correlation analyses are performed between consistency metrics and demographic or sleep variables to identify factors associated with pattern stability.
- Regression modeling is applied to identify significant predictors of subject-level consistency, quantifying the relationship between subject characteristics and sleep pattern stability.

4.1.5 Causal Inference and Confounder Adjustment

A dedicated causal module defines a Directed Acyclic Graph (DAG) representing assumed relationships between demographic factors, chronotype, sleep metrics, and cluster outcomes. Based on a specified target relationship (e.g., 'subject chronotype to cluster'), an identification function uses this DAG (leveraging the DoWhy library) to determine the minimal set of variables that need to be adjusted for to estimate the causal effect through the *Backdoor* criterion. The identified confounders are then used to construct the appropriate statistical model formula, ensuring adjustment for confounding bias.

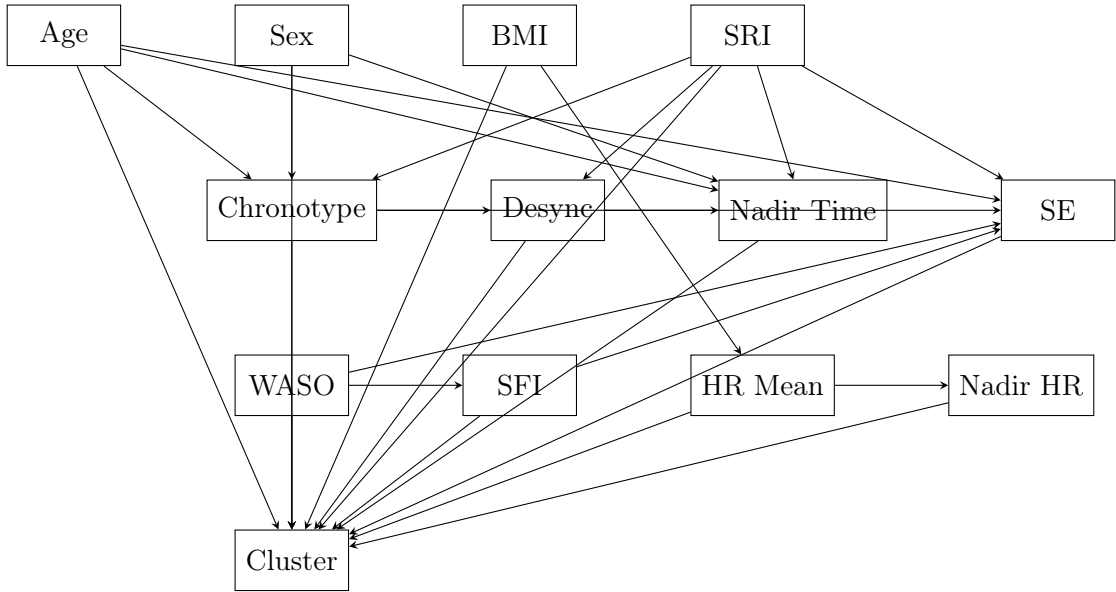


Figure 11: Directed Acyclic Graph (DAG) representing assumed causal relationships between variables. Arrows indicate direct causal effects.

4.1.6 Statistical Modeling and Visualization

A Bayesian modeling pathway is employed to assess the relationship between predictors (including the exposure variable from the target relationship and identified confounders) and the categorical cluster outcome: A multinomial mixed-effects model (`multinomial_mixed_model`) is fitted using the *Bayesian model-building interface (Bambi)*, which interfaces with PyMC for *No U-Turn Sampler (NUTS)* sampling. The model treats cluster membership as a categorical outcome (requiring casting the cluster column to string/category type), includes subject-specific random intercepts (`((1|id))`), standardizes numeric predictors, and uses Student-T non informative priors. It generates an ArviZ `InferenceData` object, allowing for detailed summary statistics (`az.summary`), assessment of parameter significance via Highest Density Intervals (HDI), posterior predictive checks (`az.plot_ppc`), convergence diagnostics (trace plots via `az.plot_trace`), and Leave-One-Out cross-validation (`az.loo`). When an initial statistical test (such as ANOVA for comparing means across multiple groups) indicates a significant overall difference, post-hoc tests (e.g., Dunn's test with p-value adjustment for multiple comparisons) are subsequently performed to identify which specific pairs of groups differ significantly from each other. These pairwise comparisons help to pinpoint the source of the overall detected effect. Model summaries, diagnostics, scaling parameters, and cross-validation results are saved. A suite of plots are produced and organized within

the `models_outputs` directory structure, categorized by analysis (e.g., posterior visualizations, effects of specific predictors like age or SRI on cluster membership), including: UMAP embeddings colored by cluster, average HR profiles per cluster, k-distance plots, coefficient plots with credible intervals, forest plots comparing effect sizes across different models/targets, and posterior density plots.

4.1.7 Parameter Tuning via Grid Search

To evaluate robustness and find optimal settings, the main script orchestrates a grid search over specified parameter ranges (e.g., `equalize_method_values`, `nadir_weight_values`, `min_clusters`, `max_clusters`). The entire pipeline is executed for each parameter combination. Results, cluster quality metrics (`n_clusters`, `noise_points`), and model diagnostics are logged to a summary file. Visual summaries of the grid search help compare performance across configurations, aiding in the selection of parameters that yield stable and meaningful results for the described clustering approach.

Summary

The pipeline constitutes an end-to-end system transforming raw sleep exam data into interpretable analyses of sleep episode patterns. Key stages involve:

- Extracting robust, physiologically motivated features (TDA vectors from HR slope dynamics and HR nadir timing).
- Aggregating features and reducing dimensionality with UMAP.
- Automatically determining the optimal number of clusters (k) and partitioning episodes using the described method (KMeans applied after determining optimal k via Silhouette analysis on nadir or UMAP data).
- Assessing subject-level cluster consistency.
- Performing in-depth inferential modeling (Bayesian multinomial models) with causal adjustment based on a predefined DAG.
- Providing extensive diagnostics and visualizations for clustering and modeling results.
- Supporting systematic parameter exploration via grid search.

This streamlined approach, focusing exclusively on the described KMeans clustering strategy, aims to uncover physiologically relevant sleep clusters derived from HR

dynamics and nadir timing, facilitating rigorous statistical interpretation and causal understanding.

5 Results

5.1 Study Population Characteristics

The study included 870 healthy individuals aged 18-75 years (mean age 46.57 ± 15.24 years), with a total of 5352 nights of recording. This resulted in 5040 valid sleep episodes used in the clustering analysis. The average number of recorded nights per individual was 6.15 nights. Table 3 summarizes key demographic and sleep characteristics of the study population.

Table 3: Descriptive Statistics of Study Population (N=870)

Characteristic	Mean \pm SD or N (%)	Range
Age (years)	46.57 ± 15.24	18-75
Sex		
Female	478 (54.9%)	–
Male	392 (45.1%)	–
BMI (kg/m^2)	24.57 ± 3.86	16.38-35.75
Total Sleep Time (min)	392.3 ± 122.0	52.2-738.7
Sleep Efficiency (%)	81.9 ± 9.6	54.6-100.0
WASO (min)	90.9 ± 46.5	0.0-285.0
SRI	70.50 ± 15.01	9.69-96.20

5.2 Clustering Outcome and Phenotype Identification

- **Cluster Identification:** The clustering method, configured to find exactly three clusters based on the TDA vector and weighted nadir timing features, successfully partitioned 5040 sleep episodes into three distinct groups. No noise points were identified, as expected from the underlying KMeans algorithm (based on clustering summary statistics).
- **Cluster Sizes:** The clusters were sized as follows: Cluster 0 (“Seahorse-like”) comprised 35.0% (1763 episodes), Cluster 1 (“Sliding Slope”) 38.2% (1923 episodes), and Cluster 2 (“Symmetric Hammock”) 26.9% (1354 episodes).
- **Cluster Validation:** The clustering quality was assessed using standard internal validation metrics. These metrics suggest a moderately good separation between the identified clusters in the feature space.
- **Driving Feature:** As indicated by the strong statistical separation and visualization (Figure 12), the primary feature driving the cluster assignment was the nadir timing percentage (`nadir_time_pct`), consistent with

the `nadir_weight=1.0` setting. The UMAP visualization (Figure 13), derived from features including both TDA characteristics and nadir timing information, showed some separation, but less distinctly than suggested by the nadir timing differences alone.

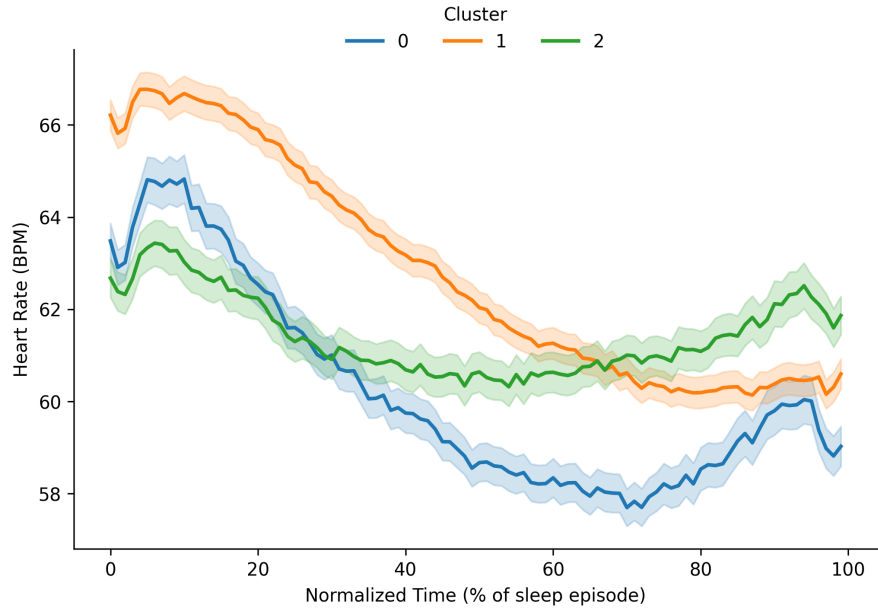


Figure 12: Average Heart Rate Profiles by Cluster. Shows distinct patterns, particularly in nadir timing, for Cluster 0 (“Seahorse-like”, Blue), Cluster 1 (“Sliding Slope”, Orange), and Cluster 2 (“Symmetric Hammock”, Green). Shaded areas represent 95% confidence intervals. The bands are calculated as follows: the Standard Error of the Mean (SEM) is computed at each time point across HR curves within a cluster (using `scipy.stats.sem`). This SEM is multiplied by 1.96 to estimate the 95% CI, due to the large sample size. The shaded region represents the mean \pm this 95% CI.

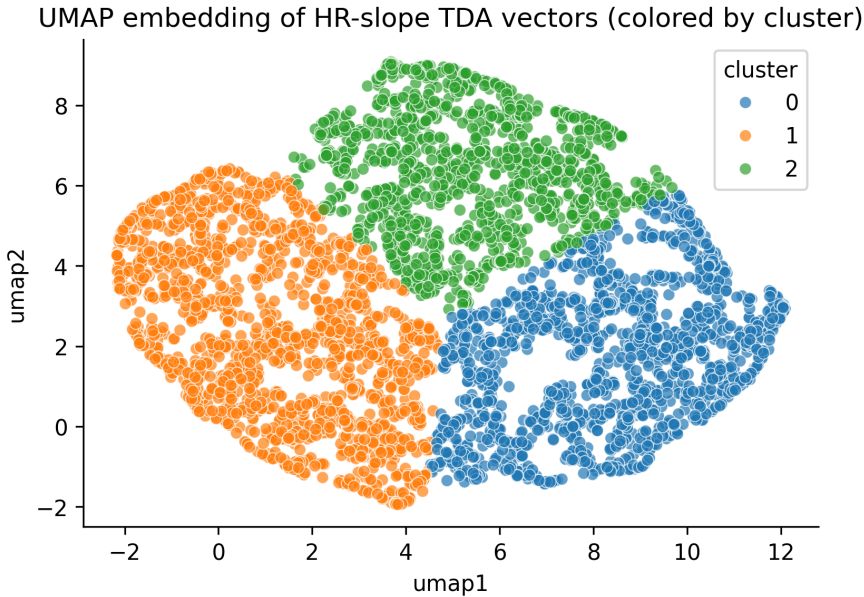


Figure 13: UMAP Embedding of Sleep Episodes Colored by Cluster. Shows partial separation of Cluster 0 (“Seahorse-like”, Blue), Cluster 1 (“Sliding Slope”, Orange), and Cluster 2 (“Symmetric Hammock”, Green) in the 2D space derived from TDA and nadir timing features.

5.3 Cluster Characterization

Inferential statistical tests (ANOVA and Chi-square) revealed significant differences between the three HR phenotypes across several variables ($p < 0.05$):

- **Nadir Timing (nadir_time_pct):** This was the most differentiating characteristic (ANOVA $p < 0.0001$), which was expected by design as the clustering methodology specifically weighted nadir timing as a key feature (with `nadir_weight=1.0`). Cluster 2 ("Symmetric Hammock") exhibited an early nadir (mean 30.7% into sleep), Cluster 0 ("Seahorse-like") a mid-period nadir (mean 69.7%), and Cluster 1 ("Sliding Slope") a late nadir (mean 81.5%). All pairwise comparisons were highly significant. Figure 17 shows the complete distributions of nadir timing for each cluster, confirming that the clusters are largely distinguished by distinct nadir timing patterns.

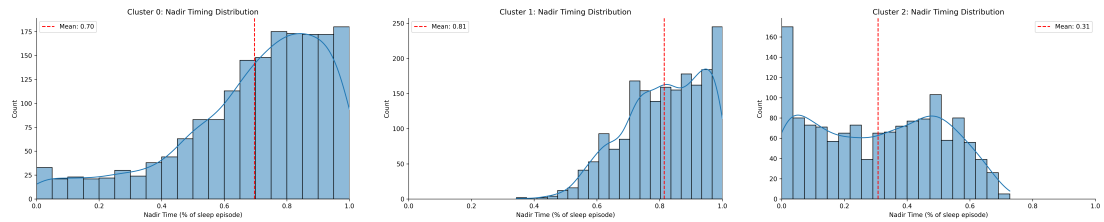


Figure 14: * Cluster 0: Mean = 0.70 Figure 15: * Cluster 1: Mean = 0.81 Figure 16: * Cluster 2: Mean = 0.31

Figure 17: Nadir Timing Distributions by Cluster. Left: Cluster 0 ("Seahorse-like") with mid-period nadir. Center: Cluster 1 ("Sliding Slope") with late nadir. Right: Cluster 2 ("Symmetric Hammock") with early nadir. The x-axis represents nadir time as a percentage of sleep episode duration.

- **Heart Rate Metrics:** Both mean episode HR (ANOVA $p < 0.0001$) and mean nadir HR (ANOVA $p < 0.0001$) differed significantly. Cluster 0 ("Seahorse-like") showed the lowest mean nadir HR (51.8 bpm) and lowest mean episode HR (60.2 bpm). Cluster 1 ("Sliding Slope") showed the highest mean nadir HR (54.7 bpm) and highest mean episode HR (62.8 bpm). Cluster 2 ("Symmetric Hammock") had intermediate values (Nadir: 53.6 bpm, Episode Mean: 61.4 bpm). Visualizations of these distributions are provided in Figure 18.

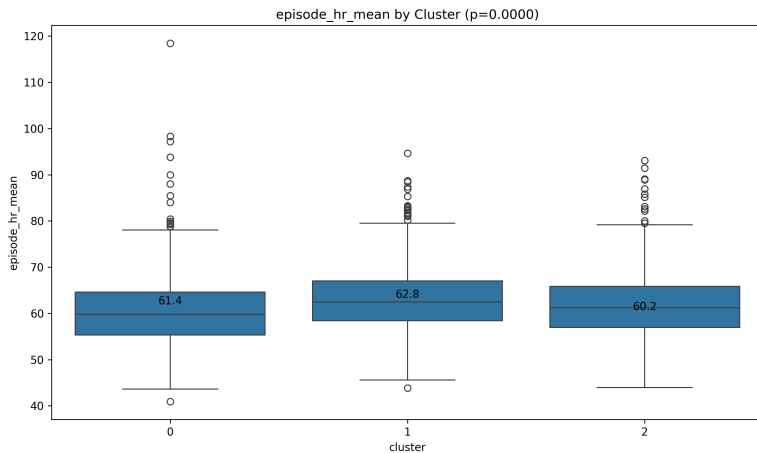


Figure 18: Distribution of Mean Episode Heart Rate by HR Phenotype Cluster.

- **Age:** A significant difference in age was observed (ANOVA $p < 0.0001$), with Cluster 0 ("Seahorse-like") participants being slightly older on average (47.5

years) compared to Cluster 2 (“Symmetric Hammock”, 45.2 years) and Cluster 1 (“Sliding Slope”, 46.3 years). Figure 19 illustrates this distribution.

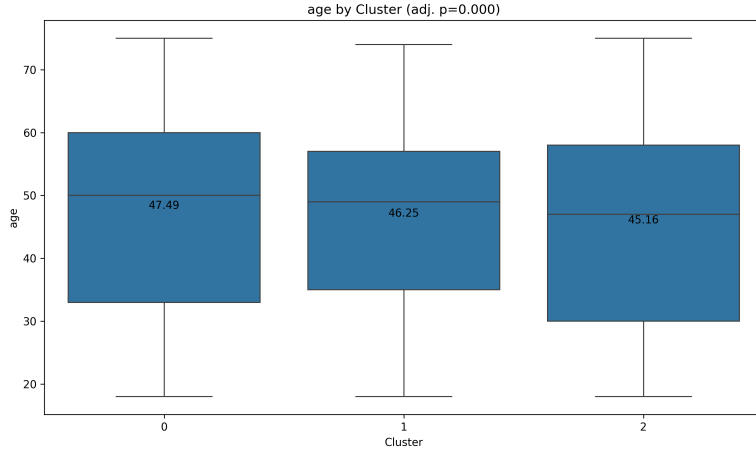


Figure 19: Distribution of Age by HR Phenotype Cluster.

- **Sex:** Cluster membership was significantly associated with sex (χ^2 p < 0.0001). Cluster 1 (“Sliding Slope”, 58.7% Female) and Cluster 2 (“Symmetric Hammock”, 59.0% Female) had notably higher proportions of females compared to Cluster 0 (“Seahorse-like”, 47.4% Female). This is detailed in Table 4 and visualized in Figure 20.

Table 4: Sex Distribution by HR Phenotype Cluster (N and %)

Cluster	Female		Male	
	N	(%)	N	(%)
Cluster 0 (“Seahorse-like”)	836	47.4%	927	52.6%
Cluster 1 (“Sliding Slope”)	1128	58.7%	795	41.3%
Cluster 2 (“Symmetric Hammock”)	799	59.0%	555	41.0%

Table 5: *

Note: Overall $\chi^2(2) = 60.026$, $p < 0.0001$. Percentages are row percentages (within each cluster).

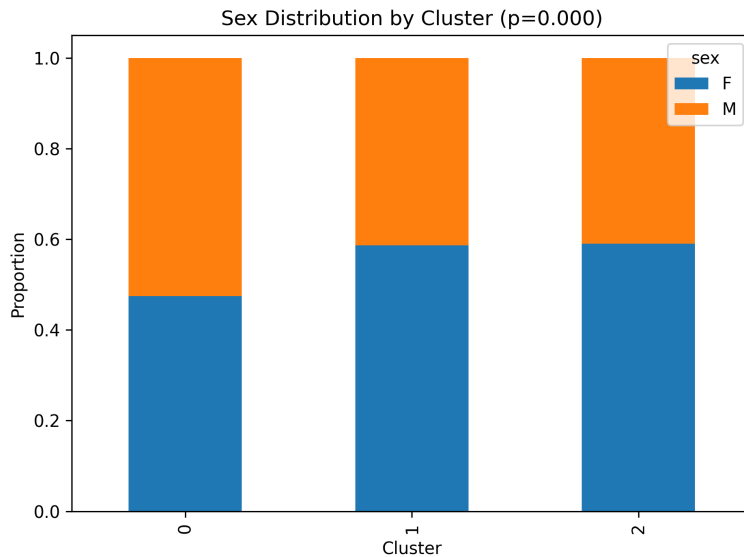


Figure 20: Proportional Sex Distribution by HR Phenotype Cluster.

- **Sleep Fragmentation Index (SFI):** SFI differed significantly (ANOVA $p < 0.0001$), with Cluster 1 (“Sliding Slope”) showing the highest fragmentation (mean 1.21) compared to Cluster 2 (“Symmetric Hammock”, mean 1.13) and Cluster 0 (“Seahorse-like”, mean 1.01).
- **Chronotype (individual_chronotype):** Significant differences were found for the individual’s average chronotype (ANOVA $p = 0.00072$). Cluster 2 (“Symmetric Hammock”) tended towards later chronotypes (mean 9.76) compared to Cluster 0 (“Seahorse-like”, mean 9.61) and Cluster 1 ("Sliding Slope", mean 9.68).
- **Absolute Chronotype Desynchronization (abs_chronotype_desync):** Significant differences were found for the absolute chronotype desynchronization (ANOVA $p = 0.0001$). Cluster 2 (“Symmetric Hammock”) had the highest absolute chronotype desynchronization (mean 1.21) compared to Cluster 0 (“Seahorse-like”, mean 1.01) and Cluster 1 ("Sliding Slope", mean 1.13).

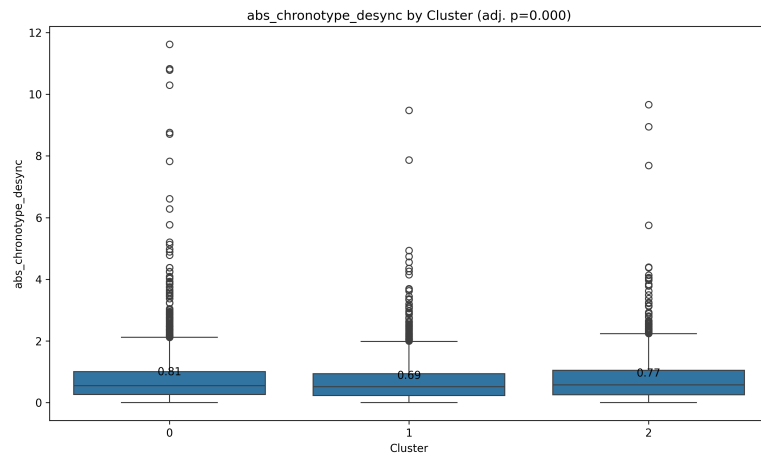


Figure 21: Distribution of Absolute Chronotype Desynchronization by HR Phenotype Cluster.

- **Wake After Sleep Onset (WASO):** WASO differed significantly (ANOVA $p = 0.0090$). Cluster 0 (“Seahorse-like”) had higher WASO (mean 91.8 min) compared to Cluster 1 (“Sliding Slope”, mean 85.7 min) and Cluster 2 (“Symmetric Hammock”, mean 86.1 min).

Variables such as sleep efficiency (SE) (ANOVA $p = 0.88$) and chronotype desynchronization (`chronotype_desync`) (ANOVA $p = 0.06$) did not show statistically significant differences across the three clusters in the initial ANOVA tests.

5.4 Heart Rate, Chronotype, and Sleep Index Interactions

Further analysis explored the intercorrelations between various heart rate (HR) metrics, chronotype variables, and sleep architecture indices. Several significant relationships ($p < 0.05$) were identified ($n=5040$ for most comparisons):

- **Chronotype Desynchronization (`chronotype_desync`):**
 - Showed a negative correlation with nadir timing percentage (`nadir_time_pct`) ($r = -0.059$, $p < 0.0001$), suggesting that greater desynchronization is associated with earlier HR nadirs.
 - Positively correlated with mean episode HR (`episode_hr_mean`) ($r = 0.075$, $p < 0.0001$) and mean nadir HR (`nadir_hr`) ($r = 0.078$, $p < 0.0001$), indicating that higher desynchronization is linked to higher overall and nadir heart rates.

- Strongly correlated with its absolute counterpart, `abs_chronotype_desync` ($r = 0.281$, $p < 0.0001$).

- **Nadir Timing Percentage (nadir_time_pct):**

- Exhibited a positive correlation with mean episode HR (`episode_hr_mean`) ($r = 0.056$, $p = 0.0001$) and mean nadir HR (`nadir_hr`) ($r = 0.031$, $p = 0.0284$), indicating later nadirs are associated with slightly higher heart rates.
- Showed a weak negative correlation with absolute chronotype desynchronization (`abs_chronotype_desync`) ($r = -0.032$, $p = 0.0219$).
- Negatively correlated with the sleep index `activity_idx` ($r = -0.049$, $p = 0.0005$), suggesting later nadirs are associated with lower activity during sleep.

- **Mean Episode HR (episode_hr_mean):**

- Showed a very strong positive correlation with mean nadir HR (`nadir_hr`) ($r = 0.905$, $p < 0.0001$), as expected.
- Positively correlated with individual chronotype (`patient_chronotype`) ($r = 0.043$, $p = 0.0021$), with later chronotypes associated with higher mean HR.
- Positively correlated with absolute chronotype desynchronization (`abs_chronotype_desync`) ($r = 0.116$, $p < 0.0001$).

- **Other Chronotype Correlations:**

- Individual chronotype (`patient_chronotype`) was positively correlated with absolute chronotype desynchronization (`abs_chronotype_desync`) ($r = 0.194$, $p < 0.0001$).
- Absolute chronotype desynchronization (`abs_chronotype_desync`) was positively correlated with mean nadir HR (`nadir_hr`) ($r = 0.057$, $p < 0.0001$).

These relationships are summarized in the correlation heatmap (Figure 22).

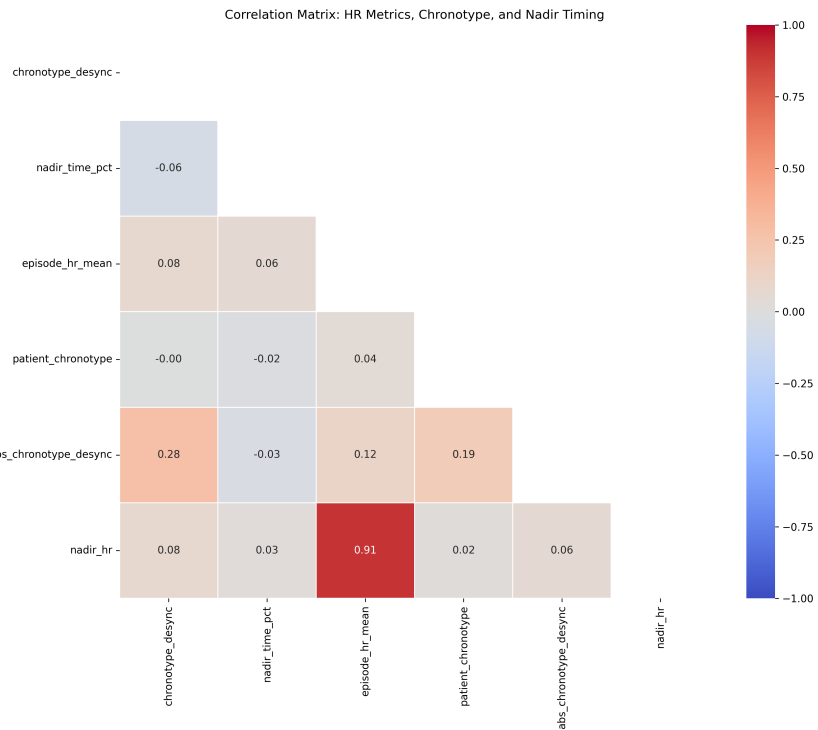


Figure 22: Correlation Heatmap of Heart Rate and Chronotype Variables. Illustrates the strength and direction of correlations between key HR metrics (nadir timing, mean episode HR, nadir HR) and chronotype-related variables (chronotype desynchronization, absolute chronotype desynchronization, patient chronotype), as well as the activity index.

5.5 Individual-Level Consistency

Analysis of cluster assignment consistency within individuals revealed considerable variability:

- **Low Overall Consistency:** The mean consistency score across individuals was low (0.17 on a scale of 0 to 1, where 1 is perfect consistency), indicating that individuals frequently exhibited different HR patterns on different nights (Figure 23). Only 5.1% of individuals showed high consistency (score > 0.8).
- **Modal Cluster Influence:** Consistency varied significantly based on the individual's most frequent (modal) cluster. Individuals whose modal pattern was Cluster 0 (“Seahorse-like”) exhibited significantly higher consistency than those predominantly in other clusters.
- **Predictors of Consistency:** A multiple regression model attempting to

predict cluster consistency based on demographic and aggregated sleep characteristics explained only a small fraction of the variance in consistency scores ($R^2 \approx 0.1$), indicating that the measured variables are not strong determinants of how consistently an individual exhibits a particular sleep pattern. The model suffered from multicollinearity (Condition Number $\approx 1.1 \times 10^6$), warranting caution in interpreting individual predictor effects.

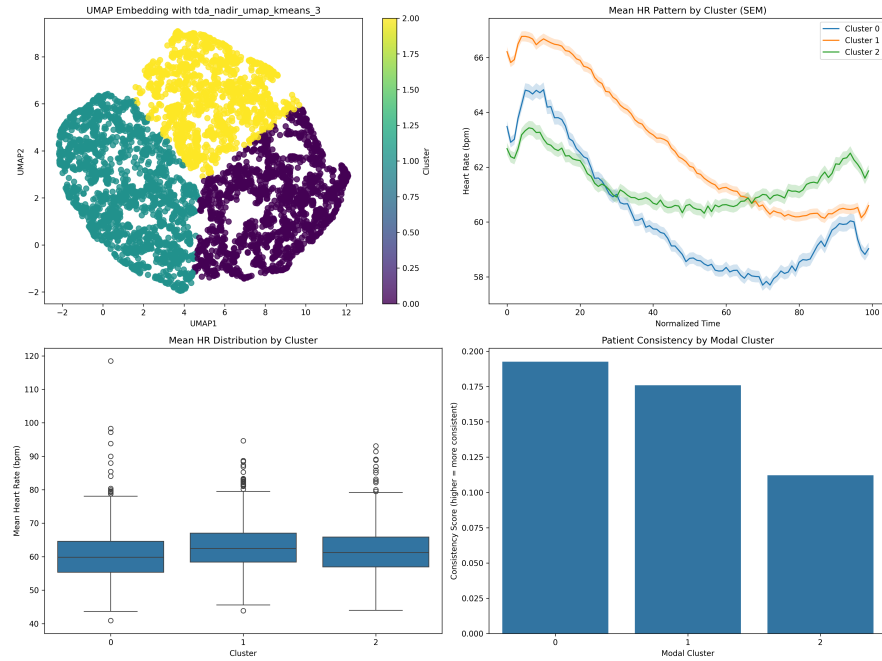


Figure 23: Distribution of Individual Cluster Consistency Scores. Shows a large peak at low consistency values, indicating high intra-individual variability in HR patterns across nights. The mean consistency score was 0.17.

5.6 Statistical Modeling of Cluster Membership

Bayesian Model Performance: The Bayesian models converged well with $R\text{-hat}$ values of approximately 1.00 across parameters and high effective sample sizes (ESS). Individual-level random intercepts showed significant variability ($\sigma \approx 0.83$, 95% HDI [0.74, 0.92]), confirming substantial baseline differences between individuals.

- **Significant Predictors (Causal Adjustment):** After adjusting for confounders identified via the DAG (Figure 11), several factors significantly predicted cluster membership:

- **Individual Chronotype:** Individual chronotype significantly predicted cluster membership (Mean effect: 0.18, 95% HDI: [0.08, 0.28], P(effect≠0): 95%). Later chronotypes were associated with increased odds of belonging to clusters with later nadir timing.
 - **Age:** Age was a significant predictor (Mean effect: -0.18, 95% HDI: [-0.28, -0.08], P(effect≠0): 95% for Cluster 2 (“Symmetric Hammock”); and Mean effect: -0.12, 95% HDI: [-0.21, -0.03], P(effect≠0): 95% for Cluster 1 (“Sliding Slope”)). Increased age was associated with reduced odds of belonging to clusters characterized by earlier HR nadirs.
 - **Sex:** Sex showed a strong relationship with cluster membership (Mean effect for males: -0.49, 95% HDI: [-0.67, -0.30], P(effect≠0): 100%). Males had significantly lower odds of belonging to clusters with earlier HR nadirs compared to females.
 - **Absolute Chronotype Desynchronization:** The magnitude of deviation from an individual’s typical chronotype significantly predicted cluster membership (Mean effect: -0.18, 95% HDI: [-0.27, -0.09], P(effect≠0): 95% for Cluster 2 (“Symmetric Hammock”); and Mean effect: -0.12, 95% HDI: [-0.21, -0.03], P(effect≠0): 95% for Cluster 1 (“Sliding Slope”)). Greater desynchronization was associated with lower odds of belonging to clusters characterized by later nadir timing.
 - **Sleep Regularity Index (SRI):** According to the posterior visualization summaries, SRI showed a significant positive association with cluster membership for certain comparisons (Mean effect: 0.14, 95% HDI: [0.04, 0.24], P(effect≠0): 95%). Higher sleep regularity was associated with increased odds of belonging to specific clusters.
 - **Sleep Efficiency (SE):** SE also showed significant associations in the posterior visualizations (Mean effect: -0.19, 95% HDI: [-0.38, -0.01], P(effect≠0): 95% for one cluster comparison). Lower sleep efficiency was associated with increased probability of specific cluster membership.
- **Non-Significant Predictors (Causal Adjustment):** One factor did not show significant relationships with cluster membership after adjustment:
 - **Raw Chronotype Desynchronization:** The directional deviation from chronotype showed weak associations with cluster membership (Mean effect: 0.03, 95% HDI: [-0.05, 0.11], P(effect≠0): 50%).

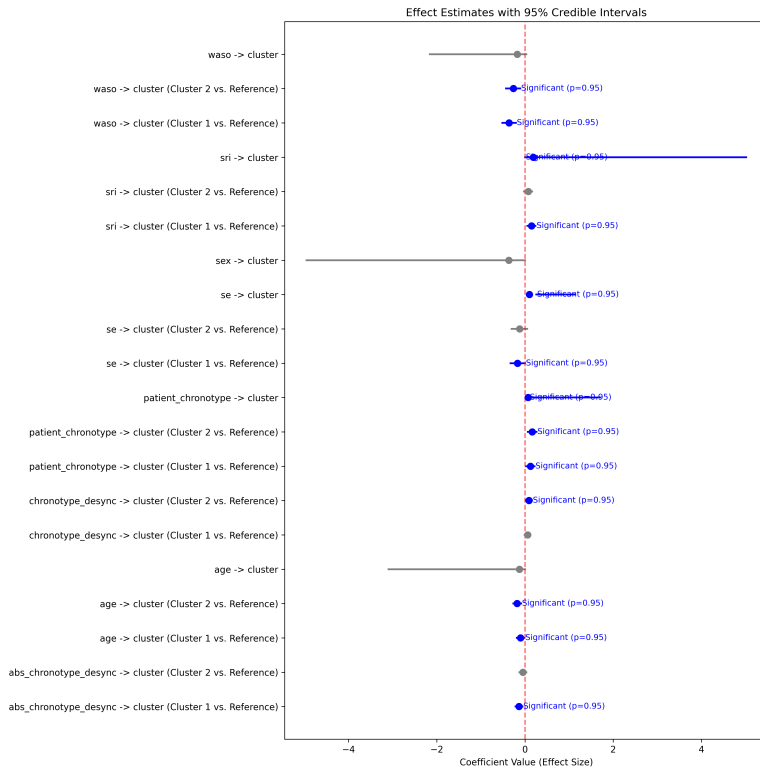


Figure 24: Forest Plot of Bayesian Model Effects on Cluster Membership. Shows the mean coefficient (dot) and 95% Highest Density Interval (line) for the effect of various predictors on the log-odds of belonging to Cluster 1 (“Sliding Slope”) or Cluster 2 (“Symmetric Hammock”) relative to Cluster 0 (“Seahorse-like”, Reference). Significant effects (HDI excludes zero) are highlighted in the plot.

5.7 Summary of Results

The analysis successfully identified three distinct HR phenotypes primarily driven by nadir timing. These phenotypes were Cluster 0 (“Seahorse-like”), Cluster 1 (“Sliding Slope”), and Cluster 2 (“Symmetric Hammock”). They differed significantly in terms of associated characteristics like age, sex distribution, sleep fragmentation, WASO, average HR levels, and average individual chronotype. Individual consistency in exhibiting a specific phenotype was generally low (mean 0.17). Bayesian causal modeling revealed several significant associations with HR phenotype patterns after adjusting for confounders: individual chronotype (effect=0.18, HDI:[0.08,0.28]), age (effect=-0.18, HDI:[-0.28,-0.08] for Cluster 2 (“Symmetric Hammock”)), sex (effect=-0.49 for males, HDI:[-0.67,-0.30]), absolute chronotype desynchronization (effect=-0.18, HDI:[-0.27,-0.09]), sleep regularity index (effect=0.14, HDI:[0.04,0.24]), and

sleep efficiency (effect=-0.19, HDI:[-0.38,-0.01]).

6 Discussion

6.1 Heart Rate Trend as a Sleep Phenotype Predictor

Cardiac research in sleep medicine has historically centered on *heart-rate variability* (HRV). Classical time-domain metrics (*RR* interval, SDNN, RMSSD, pNN50) and frequency-domain indices (LF, HF, LF/HF) dominate the literature because they map neatly onto sympatho-vagal balance. For example, Whitehurst et al., 2018 compared daytime naps with nocturnal sleep and concluded that longer night-time “cardiovascular holidays” arise from enhanced vagal tone inferred from HF power. Earlier, Trinder et al., 2001 demonstrated an abrupt shift towards parasympathetic dominance at sleep onset that remained stable within NREM stages. Subsequent clinical studies, such as Sforza et al., 2016 in idiopathic hypersomnia and Schlagintweit et al., 2023 in experimental sleep restriction, drew similar conclusions by interrogating HRV rather than the raw HR trajectory. Even reviews advocating non-linear dynamics (Penzel et al., 2003) focused on variability measures.

While invaluable, HRV reduces the complex, hour-long evolution of heart rate to statistics of variability around the mean. Mean or minimum HR values are often reported as secondary checks, and transient arousal-related spikes receive attention, but the *shape* of the overnight HR curve—the timing, steepness, and symmetry of its descent and re-ascent—has rarely entered quantitative models.

Our slope-based, TDA-driven representation fills this gap. By encoding how quickly HR falls after sleep onset and when the nadir is reached, the persistence-entropy vectors provide a stage-agnostic descriptor of sympathetic withdrawal and circadian alignment. As shown by our clusters, early versus late nadir timing captures information that HRV cannot: individuals with similar HF power can nevertheless follow radically different nocturnal trajectories. Moreover, slope features are robust to small ectopic artefacts and are readily available from any consumer wearable that delivers a continuous HR trace, circumventing the need for beat-level precision required by HRV spectral analysis.

The added dimension is not merely statistical: it offers physiological insights. A delayed nadir may reflect circadian mis-alignment or prolonged sympathetic drive, echoing findings that later nadirs predict mental-health impairment in Fudolig’s college cohort. Conversely, a steep early decline could represent efficient parasympathetic engagement that traditional HRV averages across the night would dilute.

In sum, integrating HR-slope topology with conventional HRV frames cardiovascular regulation in two complementary axes—*variability* and *trajectory*. Together they promise richer digital phenotypes for sleep research and, potentially, more sensitive biomarkers for cardiometabolic or psychiatric risk.

6.2 Topological Data Analysis in Sleep Research and Study Limitations

Topological Data Analysis (TDA) has emerged as a powerful framework for extracting shape-based information from large, noisy sleep datasets that typically defeat classical linear statistics. Applications span a range of modalities:

- **Wearable heart rate and motion.** Lee et al., 2024 combined persistent homology summaries of heart-rate and actigraphy data from Apple Watch with model-driven circadian proxies inside a neural network, improving Wake/REM/NREM classification by more than 10% over raw-signal baselines in both young and older cohorts.
- **Sleep EEG.** Persistent homology of multi-channel EEG has been used to characterise transitions between NREM sub-stages and to flag pathological connectivity patterns in sleep apnoea Manjunath et al., 2023.
- **Cardiovascular dynamics.** Shape-based analyses of the overnight heart-rate curve have proved informative. Our present study applies TDA to persistence summaries of HR slopes, whereas Fudolig et al., 2024 used classical time-series clustering (PAA + k -means) without TDA to isolate two canonical curve shapes.

Where previous work falls short. While these studies demonstrate the value of shape-based features, their scope and design impose important constraints:

- **Reliance on summary indices (Katori et al., 2022).** Katori and colleagues clustered 103,200 wrist-accelerometer recordings from the UK Biobank with UMAP + DBSCAN, but the feature space was restricted to classical sleep indices (duration, timing, efficiency). Without physiological signals such as heart rate or TDA descriptors, phenotype assignment rested on proxies that ignore internal cardiovascular dynamics, potentially misclassifying “late” versus “early” types and masking intra-individual variability.
- **Homogeneous convenience sample (Fudolig et al., 2024).** The LEMURS study extracted two canonical shapes of the sleep heart-rate curve from 25,800 nights in about 600 first-year U.S. college students, linking later nadirs to poorer mental-health indicators. Although methodologically rigorous (meta-clustering + logistic regression), the narrow age range and shared campus environment limit external validity; effects may differ in older adults, shift-workers, or clinical groups.
- **Black-box neural pipelines (Lee et al., 2024).** The performance gains

achieved by combining TDA with deep learning come at the cost of interpretability, and the algorithm was evaluated on overnight polysomnography rather than free-living multi-night data.

Contribution of the present study. We address these gaps by: (i) deriving persistence-entropy vectors from the slope of the heart-rate curve itself, capturing micro-fluctuations ignored by nadir timing alone; (ii) analysing 5040 nights from 870 healthy adults spanning a wider age distribution, thus bridging the demographic gap between the homogeneous LEMURS cohort and the older UK Biobank sample; and (iii) integrating chronotype, sleep regularity, and causal Bayesian modelling to disentangle demographic from behavioural drivers of HR shape. Our findings therefore extend TDA-based phenotyping to a population-level yet individually repeated design, offering a scalable reference framework for future clinical or interventional studies.

Future research should now combine the complementary strengths of existing approaches—large, diverse cohorts (Katori), interpretable cardiovascular descriptors (the present work), and multimodal TDA-augmented machine learning (Lee) to build robust digital biomarkers that generalise across devices, demographics, and clinical settings.

6.3 Summary of Principal Findings

This study successfully employed a comprehensive pipeline, integrating features derived from Topological Data Analysis (TDA) of heart rate (HR) slope dynamics with HR nadir timing characteristics, to analyze HR dynamics during sleep. From 5040 sleep episodes in 870 healthy individuals, three distinct HR phenotypes were identified using a clustering approach applied to a feature set that included both TDA vectors and nadir timing information yielding:

- Cluster 0 ("Seahorse-like"): Characterized by a mid-period HR nadir, lower mean and nadir HR, slightly older individuals, a higher proportion of males, lower sleep fragmentation.
- Cluster 1 ("Sliding Slope"): Defined by a late HR nadir, the highest mean and nadir HR, a higher proportion of females, and the highest sleep fragmentation.
- Cluster 2 ("Symmetric Hammock"): Exhibited an earlier HR nadir, intermediate HR metrics, a higher proportion of females, earlier chronotypes.

Significant differences across these phenotypes were observed for age, sex, Sleep Fragmentation Index (SFI), individual chronotype, absolute chronotype desynchronization, and Wake After Sleep Onset (WASO). However, individual-level

consistency in exhibiting a specific phenotype was generally low (mean consistency score of 0.17). Bayesian multinomial mixed-effects modeling, with confounder adjustment guided by a Directed Acyclic Graph (DAG), identified several significant predictors of cluster membership. These included individual chronotype, age, sex, absolute chronotype desynchronization, Sleep Regularity Index (SRI), and Sleep Efficiency (SE).

6.4 Interpretation of Findings

The identification of three distinct HR phenotypes, primarily differentiated by their nadir timing, aligns with the study's aim to uncover sleep patterns based on HR characteristics. The "Seahorse-like," "Sliding Slope," and "Symmetric Hammock" patterns suggest that the timing of the lowest heart rate during sleep is a key physiological differentiator. The association of these phenotypes with demographic factors like age and sex, as well as sleep architecture variables like SFI and WASO, and chronotype measures, underscores their potential physiological relevance. For instance, the older age profile and lower SFI in the "Seahorse-like" group, or the higher SFI in the "Sliding Slope" group, point towards complex interactions between HR dynamics, sleep quality, and aging.

their individual role in defining the final cluster separation was less prominent in this specific configuration. This observation is supported by the UMAP visualizations presented in the results (Figure 13), which, although derived from the combined feature set including TDA vectors, showed more modest inter-cluster separation compared to the distinctions driven by nadir timing alone. This suggests that with the current weighting, nadir timing emerged as a more dominant feature for this particular HR-based sleep phenotyping.

The low intra-individual consistency in phenotype expression is a critical finding. It suggests that while these HR patterns are observable across a population, an individual may not consistently exhibit the same pattern nightly. This variability could reflect normal physiological fluctuations, responses to daily behavioral changes (e.g., stress, activity levels, meal timing), or intrinsic instability in sleep HR regulation for many individuals. This finding has implications for the concept of stable, long-term sleep "types" based solely on nightly HR patterns.

The Bayesian modeling results, adjusted for confounding, provide insights into factors associated with these HR patterns. The significance of individual chronotype, age, and sex aligns with known influences on cardiovascular function and sleep regulation. The link with SRI and SE further suggests that regularity and quality of sleep are intertwined with specific HR dynamic patterns. The negative association of absolute chronotype desynchronization with later nadir clusters implies that deviations from one's typical sleep timing may shift HR patterns towards earlier nadirs.

6.5 Limitations of the Study

Despite its strengths, this study has several limitations:

- **Dominance of Nadir Timing:** While the strong influence of nadir timing in clustering was by design, it may have overshadowed other subtle HR dynamic features potentially captured by TDA. The UMAP visualizations showed only partial separation, suggesting that the feature space beyond nadir timing might be complex.
- **Low Individual Consistency:** The low intra-individual consistency in phenotype membership poses a challenge for interpreting these clusters as stable individual traits. The factors driving this nightly variability were not fully elucidated by the regression model for consistency, which had low explanatory power ($R^2 \approx 0.1$) and suffered from multicollinearity.
- **Healthy Population:** The study cohort consisted of healthy individuals. The findings regarding HR phenotypes and their correlates may not be directly generalizable to clinical populations with sleep disorders or cardiovascular conditions.
- **Assumed DAG Structure:** The causal inferences are contingent upon the correctness of the predefined DAG. While theory-driven, the DAG represents assumed relationships, and alternative causal structures could exist.
- **Interpretability of TDA Features:** While mathematically robust, the direct physiological interpretation of TDA vectors (persistence entropy from HR slope) can be less intuitive than traditional HR metrics.

6.6 Future Research Directions

Building upon the current findings and limitations, future research could explore several avenues:

- **Investigating Intra-Individual Variability:** Further studies are needed to understand the drivers of low consistency in nightly HR phenotype expression. This could involve collecting more granular data on daily behaviors, environmental factors, and stress levels.
- **Exploring Alternative Feature Weighting and Clustering:** Experimenting with different clustering selection values or using clustering algorithms that can better utilize the TDA features might reveal different or more nuanced sleep phenotypes. Meta-clustering or ensemble approaches could also be considered.

- **Clinical Populations:** Applying this methodology to clinical populations (e.g., patients with insomnia, sleep apnea, or cardiovascular diseases) could identify clinically relevant HR phenotypes and assess their diagnostic or prognostic value.
- **Longitudinal Studies:** Tracking HR phenotypes and their consistency over longer periods (months or years) would provide insights into their stability and potential changes with age or health status.
- **Refining Causal Models:** Future work could involve refining the DAG based on new evidence or using methods for causal discovery to learn aspects of the causal structure from data.
- **Multimodal Data Integration:** Integrating other physiological signals (e.g., respiration, movement, EEG-derived sleep stages if available) could provide a more holistic understanding of sleep states beyond HR dynamics.

6.7 Conclusion

This study successfully identified three distinct sleep HR phenotypes in a large, healthy cohort, primarily characterized by differences in HR nadir timing. These phenotypes showed significant associations with demographic, chronobiological, and sleep quality metrics. Bayesian modeling, with causal adjustment, highlighted individual chronotype, age, sex, chronotype desynchronization, SRI, and SE as important factors related to phenotype membership. While the identified phenotypes provide valuable insights into population-level HR patterns during sleep, the observed low intra-individual consistency suggests that nightly HR dynamics are highly variable within individuals. Future research should focus on understanding this variability and exploring the clinical utility of these HR-based sleep phenotypes. The comprehensive methodological pipeline developed offers a robust framework for such future investigations.

7 Appendix

7.1 Online Material



Figure 25: QR code linking to the online repository containing supplementary materials and code (url: <https://github.com/f-starace/hr-tda>)

7.2 Supplementary Figures and Tables

7.2.1 Clustering Parameters

The following table summarizes the key parameters used for the clustering analysis described in Section 3.

Table 6: Clustering Parameters

Parameter	Value
equalize_method	resample
eps	0.4
min_samples	5
nadir_weight	0.5
use_causal	True
causal_exposure	None
prior_type	student_t
prior_scale	2.0
clustering_algorithm	tda_nadir_umap_kmeans_3
cv_method	loo
min_clusters	2
max_clusters	10
favor_higher_k	True
penalty_weight	0.05
reduced_mcmc	False

7.2.2 Overall Clustering Statistics

The table below provides a summary of the clustering results.

Table 7: Overall Clustering Statistics

Metric	Value
Number of clusters	3
Noise points	0 (0.0%)
Cluster 0 size	1763 (35.0%)
Cluster 1 size	1923 (38.2%)
Cluster 2 size	1354 (26.9%)
Mean Consistency	0.17
% Patients >0.8 Consistency	5.1
Mean Modal Proportion	0.62

7.2.3 Heart Rate Statistics by Cluster

The following figure shows boxplots of various heart rate statistics, grouped by cluster.

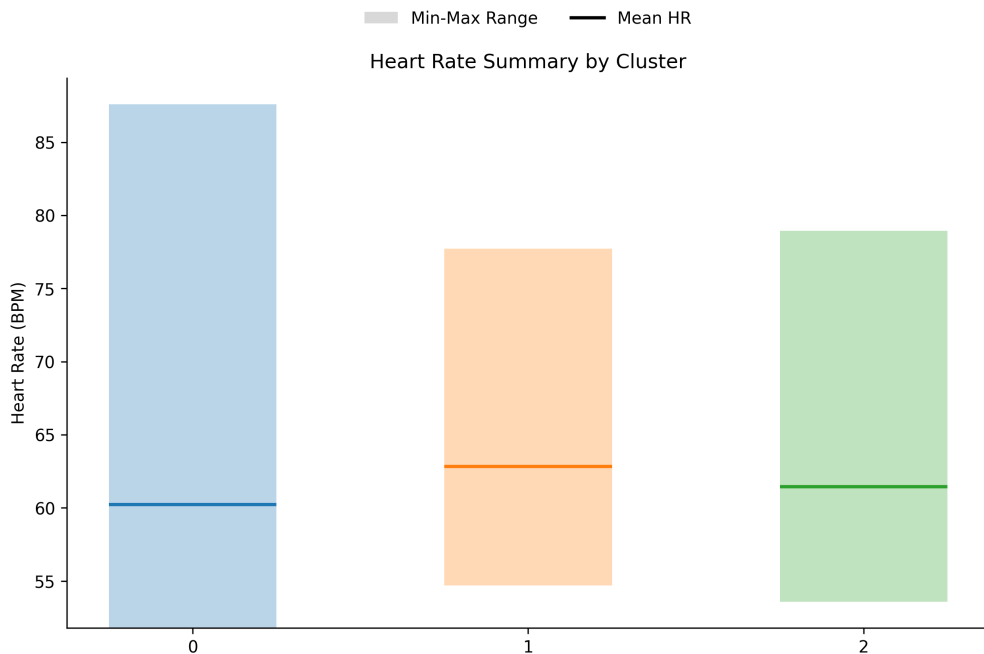


Figure 26: Heart Rate Statistics by Cluster. Boxplots showing distributions of Mean HR, Nadir HR, and Nadir Time Pct for each identified cluster.

7.2.4 Individual Cluster Heart Rate Profiles

The figures below show the average heart rate curves for each cluster individually, providing a more detailed view of the HR dynamics within each phenotype.

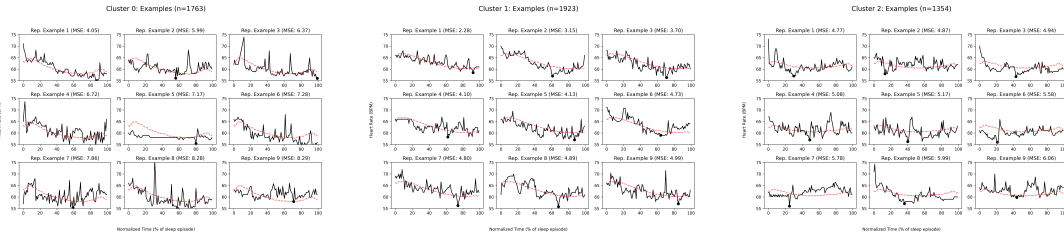


Figure 27: *
Cluster 0 HR Profile

Figure 28: *
Cluster 1 HR Profile

Figure 29: *
Cluster 2 HR Profile

Figure 30: Individual Average Heart Rate Profiles by Cluster.

7.2.5 Detailed Cluster Statistics

Statistical comparison of clusters (cluster)

Table 8: Post-hoc Dunn test for age (p-values)

Cluster	0	1	2
0	1.000000	0.001976	0.000016
1	0.001976	1.000000	0.127646
2	0.000016	0.127646	1.000000

Post-hoc Dunn test for age

ANOVA for age F-statistic: 9.370, p-value: 0.00009

Significant difference in age between clusters

Table 9: Mean age by cluster

Cluster	Mean Age	Std. Dev.
0	47.494044	15.655715
1	46.254290	14.278460
2	45.157312	15.292359

Means for age by cluster

Table 10: Post-hoc Dunn test for patient_chronotype (p-values)

Cluster	0	1	2
0	1.000000	0.039841	0.000006
1	0.039841	1.000000	0.007096
2	0.000006	0.007096	1.000000

Post-hoc Dunn test for patient_chronotype

ANOVA for patient_chronotype F-statistic: 7.240, p-value: 0.00072
Significant difference in patient_chronotype between clusters

Table 11: Mean patient_chronotype by cluster

Cluster	Mean Chronotype	Std. Dev.
0	9.610619	1.106658
1	9.680760	1.119260
2	9.762687	1.087907

Means for patient_chronotype by cluster

ANOVA for se F-statistic: 0.124, p-value: 0.88357

Table 12: Post-hoc Dunn test for WASO (p-values)

Cluster	0	1	2
0	1.000000	0.000037	0.000518
1	0.000037	1.000000	0.763550
2	0.000518	0.763550	1.000000

Post-hoc Dunn test for waso

ANOVA for waso F-statistic: 4.712, p-value: 0.00903

Significant difference in WASO between clusters

Table 13: Mean WASO by cluster

Cluster	Mean WASO	Std. Dev.
0	91.815655	63.320120
1	85.727509	66.811090
2	86.110783	66.387435

Means for WASO by cluster

Table 14: Post-hoc Dunn test for SFI (p-values)

Cluster	0	1	2
0	1.000000e+00	5.436857e-18	0.000004
1	5.436857e-18	1.000000e+00	0.000869
2	3.867529e-06	8.692204e-04	1.000000

Post-hoc Dunn test for sfi

ANOVA for sfi F-statistic: 43.137, p-value: 0.00000

Significant difference in SFI between clusters

Table 15: Mean SFI by cluster

Cluster	Mean SFI	Std. Dev.
0	1.011611	0.588473
1	1.212101	0.702169
2	1.128213	0.670919

Means for SFI by cluster

Table 16: Post-hoc Dunn test for nadir_time_pct (p-values)

Cluster	0	1	2
0	1.000000e+00	3.282125e-41	1.005442e-279
1	3.282125e-41	1.000000e+00	0.000000e+00
2	1.005442e-279	0.000000e+00	1.000000e+00

Post-hoc Dunn test for nadir_time_pct

ANOVA for nadir_time_pct F-statistic: 2896.631, p-value: 0.00000
Significant difference in nadir_time_pct between clusters

Table 17: Mean nadir_time_pct by cluster

Cluster	Mean nadir_time_pct	Std. Dev.
0	0.696551	0.236998
1	0.814662	0.127779
2	0.307238	0.203223

Means for nadir_time_pct by cluster

Table 18: Post-hoc Dunn test for nadir_hr (p-values)

Cluster	0	1	2
0	1.000000e+00	2.229601e-43	4.650909e-15
1	2.229601e-43	1.000000e+00	1.211860e-06
2	4.650909e-15	1.211860e-06	1.000000e+00

Post-hoc Dunn test for nadir_hr

ANOVA for nadir_hr F-statistic: 95.734, p-value: 0.00000
Significant difference in nadir_hr between clusters

Table 19: Mean nadir_hr by cluster

Cluster	Mean nadir_hr	Std. Dev.
0	51.794162	6.584133
1	54.692898	6.089313
2	53.570454	6.517867

Means for nadir_hr by cluster

Table 20: Post-hoc Dunn test for episode_hr_mean (p-values)

Cluster	0	1	2
0	1.000000e+00	2.536968e-32	2.096080e-07
1	2.536968e-32	1.000000e+00	1.103281e-08
2	2.096080e-07	1.103281e-08	1.000000e+00

Post-hoc Dunn test for episode_hr_mean

ANOVA for episode_hr_mean F-statistic: 70.054, p-value: 0.00000
Significant difference in episode_hr_mean between clusters

Table 21: Mean episode_hr_mean by cluster

Cluster	Mean episode_hr_mean	Std. Dev.
0	60.200275	7.028803
1	62.824304	6.477788
2	61.446239	6.687930

Means for episode_hr_mean by cluster

ANOVA for chronotype_desync F-statistic: 2.770, p-value: 0.06278

Chi-square test for sex Chi2 = 60.026, p-value: 0.00000, dof: 2
Significant association between sex and cluster

Table 22: Sex contingency table

Cluster	F	M
0	836	927
1	1128	795
2	799	555

Contingency table

Table 23: Proportions by sex and cluster

Cluster	F	M
0	47.419172	52.580828
1	58.658346	41.341654
2	59.010340	40.989660

Proportions

8 Acknowledgements

I wish to express my sincere gratitude to my supervisor, Professor Faraguna, for his insightful guidance and support throughout the course of this research.

My heartfelt thanks are also extended to my family and friends for their constant encouragement, patience, and understanding during this journey.

Finally, I would like to thank Sleepacta S.R.L. for generously providing the data that formed the basis of this study.

References

- Zheng, N. S., Annis, J., Master, H., Han, L., Gleichauf, K., Ching, J. H., Nasser, M., Coleman, P., Desine, S., Ruderfer, D. M., Hernandez, J., Schneider, L. D., & Brittain, E. L. (2024). Sleep patterns and risk of chronic disease as measured by long-term monitoring with commercial wearable devices in the all of us research program. *Nature Medicine*, 30(9), 2648–2656. <https://doi.org/10.1038/s41591-024-03155-8>
- Li, H.-M., Zhang, X.-R., Liao, D.-Q., Gao, J., Qiu, C.-S., Zhong, W.-F., Tang, X.-L., Chen, P.-L., Du, L.-Y., Yang, J., Lai, S.-M., Huang, Q.-M., Wang, X.-M., Song, W.-Q., You, F.-F., Li, C., Shen, D., Mao, C., & Li, Z.-H. (2025). Healthy sleep patterns and risk of hospitalization for infection: A large community-based cohort study. *Translational Psychiatry*, 15(1), 100. <https://doi.org/10.1038/s41398-025-03314-6>
- Xie, L., Kang, H., Xu, Q., Chen, M. J., Liao, Y., Thiagarajan, M., O'Donnell, J., Christensen, D. J., Nicholson, C., Iliff, J. J., Takano, T., Deane, R., & Nedergaard, M. (2013). Sleep drives metabolite clearance from the adult brain. *Science*, 342(6156), 373–377. <https://doi.org/10.1126/science.1241224>
- Mittermaier, F. X., Kalbhenn, T., Xu, R., Onken, J., Faust, K., Sauvigny, T., Thomale, U. W., Kaindl, A. M., Holtkamp, M., Grosser, S., Fidzinski, P., Simon, M., Alle, H., & Geiger, J. R. P. (2024). Membrane potential states gate synaptic consolidation in human neocortical tissue. *Nature Communications*, 15(1), 10340. <https://doi.org/10.1038/s41467-024-53901-2>
- Glosemeyer, R. W., Diekelmann, S., Cassel, W., Kesper, K., Koehler, U., Westermann, S., Steffen, A., Borgwardt, S., Wilhelm, I., Müller-Pinzler, L., Paulus, F. M., Krach, S., & Stoltz, D. S. (2020). Selective suppression of rapid eye movement sleep increases next-day negative affect and amygdala responses to social exclusion. *Scientific Reports*, 10(1), 17325. <https://doi.org/10.1038/s41598-020-74169-8>
- Roenneberg, T., Wirz-Justice, A., & Merrow, M. (2003). Life between clocks: Daily temporal patterns of human chronotypes [PMID: 12568247]. *Journal of Biological Rhythms*, 18(1), 80–90. <https://doi.org/10.1177/0748730402239679>
- Jankowski, K. S., Fajkowska, M., Domaradzka, E., & Wytykowska, A. (2019). Chronotype, social jetlag and sleep loss in relation to sex steroids. *Psychoneuroendocrinology*, 108, 87–93. <https://doi.org/https://doi.org/10.1016/j.psyneuen.2019.05.027>
- Pandi-Perumal, S. R., Smits, M., Spence, W., Srinivasan, V., Cardinali, D. P., Lowe, A. D., & Kayumov, L. (2007). Dim light melatonin onset (dlmo): A tool for the analysis of circadian phase in human sleep and chronobiological

- disorders. *Progress in Neuro-Psychopharmacology and Biological Psychiatry*, 31(1), 1–11. [https://doi.org/https://doi.org/10.1016/j.pnpbp.2006.06.020](https://doi.org/10.1016/j.pnpbp.2006.06.020)
- Burgess, H. J., Kikyo, F., Valdespino-Hayden, Z., Rizvydeen, M., Kimura, M., Pollack, M. H., Hobfoll, S. E., Rajan, K. B., Zalta, A. K., & Burns, J. W. (2018). Do the morningness-eveningness questionnaire and munich chronotype questionnaire change after morning light treatment? *Sleep Science and Practice*, 2(1), 12. <https://doi.org/10.1186/s41606-018-0031-1>
- Reiter, A. M., Sargent, C., & Roach, G. D. (2021). Concordance of chronotype categorisations based on dim light melatonin onset, the morningness-eveningness questionnaire, and the munich chronotype questionnaire. *Clocks & Sleep*, 3(2), 342–350. <https://doi.org/10.3390/clockssleep3020021>
- Horne, J., & Ostberg, O. (1976). A self assessment questionnaire to determine morningness eveningness in human circadian rhythms. *International journal of chronobiology*, 4, 97–110.
- Di Milia, L., Adan, A., Natale, V., & Randler, C. (2013). Reviewing the psychometric properties of contemporary circadian typology measures [PMID: 24001393]. *Chronobiology International*, 30(10), 1261–1271. <https://doi.org/10.3109/07420528.2013.817415>
- Suh, S., Ryu, H., Kim, S., Choi, S., & Joo, E. Y. (2017). Using mid-sleep time to determine chronotype in young adults with insomnia-related symptoms. *Sleep Med Res*, 8(2), 107–111. <https://doi.org/10.17241/smr.2017.00115>
- Roenneberg, T. (2023). How can social jetlag affect health? *Nature Reviews Endocrinology*, 19(7), 383–384. <https://doi.org/10.1038/s41574-023-00851-2>
- Wei, Y., Wang, S., Wang, W., & and, X. L. (2024). Using actigraphy to assess chronotype: Simpler is better [PMID: 39569655]. *Chronobiology International*, 41(11), 1469–1479. <https://doi.org/10.1080/07420528.2024.2428196>
- Schneider, J., Fárová, E., & and, E. B. (2022). Human chronotype: Comparison of questionnaires and wrist-worn actigraphy [PMID: 34806526]. *Chronobiology International*, 39(2), 205–220. <https://doi.org/10.1080/07420528.2021.1992418>
- Fischer, D., Lombardi, D. A., Marucci-Wellman, H., & Roenneberg, T. (2017). Chronotypes in the us - influence of age and sex. *PLOS ONE*, 12(6), 1–17. <https://doi.org/10.1371/journal.pone.0178782>
- Natale, V., Esposito, M. J., Martoni, M., & Fabbri, M. (2006). Validity of the reduced version of the morningness-eveningness questionnaire. *Sleep and Biological Rhythms*, 4(1), 72–74. <https://doi.org/10.1111/j.1479-8425.2006.00192.x>
- Roenneberg, T., Kuehnle, T., Juda, M., Kantermann, T., Allebrandt, K., Gordijn, M., & Merrow, M. (2007). Epidemiology of the human circadian clock. *Sleep*

- Medicine Reviews*, 11(6), 429–438. [https://doi.org/https://doi.org/10.1016/j.smrv.2007.07.005](https://doi.org/10.1016/j.smrv.2007.07.005)
- Randler, C., & Engelke, J. (2019). Gender differences in chronotype diminish with age: A meta-analysis based on morningness/chronotype questionnaires. *Chronobiology International*, 36(7), 888–905. <https://doi.org/10.1080/07420528.2019.1585867>
- Steven, D., Lombardi, D., Marucci-Wellman, H., & Roenneberg, T. (2017). Chronotypes in the us - influence of age and sex. *PLOS ONE*, 12, e0178782. <https://doi.org/10.1371/journal.pone.0178782>
- McCall, C., Duncan, G., & Watson, N. (2021). Twin studies in sleep medicine: A review. *Medical Research Archives*, 9(7). <https://doi.org/10.18103/mra.v9i7.2471>
- Kalmbach, D. A., Schneider, L. D., Cheung, J., Bertrand, S. J., Kariharan, T., Pack, A. I., & Gehrman, P. R. (2016). Genetic basis of chronotype in humans: Insights from three landmark gwas. *Sleep*, 40(2), zsw048. <https://doi.org/10.1093/sleep/zsw048>
- Pavithra, S., Aich, A., Chanda, A., Zohra, I. F., Gawade, P., & Das, R. K. (2024). Per2 gene and its association with sleep-related disorders: A review. *Physiology & Behavior*, 273, 114411. <https://doi.org/https://doi.org/10.1016/j.physbeh.2023.114411>
- Jankowski, K. S. (2017). Social jet lag: Sleep-corrected formula [PMID: 28318321]. *Chronobiology International*, 34(4), 531–535. <https://doi.org/10.1080/07420528.2017.1299162>
- Wittmann, M., Dinich, J., Merrow, M., & Roenneberg, T. (2006). Social jetlag: Misalignment of biological and social time. *Chronobiology International*, 23(1-2), 497–509. <https://doi.org/10.1080/07420520500545979>
- Caliandro, R., Streng, A. A., van Kerkhof, L. W. M., van der Horst, G. T. J., & Chaves, I. (2021). Social jetlag and related risks for human health: A timely review. *Nutrients*, 13(12). <https://doi.org/10.3390/nu13124543>
- Koopman, A. D., Rauh, S. P., vant Riet, E., Groeneveld, L., van der Heijden, A. A., Elders, P. J., Dekker, J. M., Nijpels, G., Beulens, J. W., & Rutters, F. (2017). The association between social jetlag, the metabolic syndrome, and type 2 diabetes mellitus in the general population: The new hoorn study [PMID: 28631524]. *Journal of Biological Rhythms*, 32(4), 359–368. <https://doi.org/10.1177/0748730417713572>
- Shafer, B. M., McAuliffe, K. E., & McHill, A. W. (2023). A longitudinal look at social jetlag, sex differences, and obesity risk. *Sleep*, 47(1), zsad298. <https://doi.org/10.1093/sleep/zsad298>
- Driller, M., Dunican, I. C., Omund, S., Boukhris, O., Stevenson, S., Lambing, K., & Bender, A. (2023). Pyjamas, polysomnography and professional athletes:

- The role of sleep tracking technology in sport. *Sports*, 11. <https://doi.org/10.3390/sports11010014>
- Morris, C. J., Aeschbach, D., & Scheer, F. A. (2012). Circadian system, sleep and endocrinology [The role of circadian clock in endocrinology]. *Molecular and Cellular Endocrinology*, 349(1), 91–104. <https://doi.org/https://doi.org/10.1016/j.mce.2011.09.003>
- Dibner, C., Schibler, U., & Albrecht, U. (2010). The mammalian circadian timing system: Organization and coordination of central and peripheral clocks. *Annual Review of Physiology*, 72(Volume 72, 2010), 517–549. <https://doi.org/https://doi.org/10.1146/annurev-physiol-021909-135821>
- Berson, D. M. (2003). Strange vision: Ganglion cells as circadian photoreceptors. *Trends in Neurosciences*, 26(6), 314–320. [https://doi.org/https://doi.org/10.1016/S0166-2236\(03\)00130-9](https://doi.org/https://doi.org/10.1016/S0166-2236(03)00130-9)
- Boudreau, P., Yeh, W.-H., Dumont, G. A., & Boivin, D. B. (2013). Circadian variation of heart rate variability across sleep stages. *Sleep*, 36(12), 1919–1928. <https://doi.org/10.5665/sleep.3230>
- Sforza, E., Roche, F., Barthélémy, J. C., & Pichot, V. (2016). Diurnal and nocturnal cardiovascular variability and heart rate arousal response in idiopathic hypersomnia. *Sleep Medicine*, 24, 131–136. <https://doi.org/https://doi.org/10.1016/j.sleep.2016.07.012>
- Burgess, H. J., Trinder, J., Kim, Y., & Luke, D. (1997). Sleep and circadian influences on cardiac autonomic nervous system activity [PMID: 9362241]. *American Journal of Physiology-Heart and Circulatory Physiology*, 273(4), H1761–H1768. <https://doi.org/10.1152/ajpheart.1997.273.4.H1761>
- Trinder, J., Kleiman, J., Carrington, M., Smith, S., Breen, S., Tan, N., & Kim, Y. (2001). Autonomic activity during human sleep as a function of time and sleep stage. *Journal of Sleep Research*, 10(4), 253–264. <https://doi.org/http://doi.org/10.1046/j.jsr.2001.00263.x>
- Cosgrave, J., Phillips, J., Haines, R., Foster, R. G., Steinsaltz, D., & Wulff, K. (2021). Revisiting nocturnal heart rate and heart rate variability in insomnia: A polysomnography-based comparison of young self-reported good and poor sleepers. *Journal of Sleep Research*, 30(4), e13278. <https://doi.org/https://doi.org/10.1111/jsr.13278>
- Natarajan, A., Gleichauf, K., Khalid, M., Heneghan, C., & Schneider, L. D. (2025). Circadian rhythm of heart rate and activity: A cross-sectional study [Epub 2025-01-14]. *Chronobiology International*, 42(1), 108–121. <https://doi.org/10.1080/07420528.2024.2446622>
- Borbély, A. A., Daan, S., Wirz-Justice, A., & Deboer, T. (2016). The two-process model of sleep regulation: A reappraisal. *Journal of Sleep Research*, 25(2), 131–143. <https://doi.org/https://doi.org/10.1111/jsr.12371>

- Franken, P., & Dijk, D.-J. (2024). Sleep and circadian rhythmicity as entangled processes serving homeostasis. *Nature Reviews Neuroscience*, 25(1), 43–59. <https://doi.org/10.1038/s41583-023-00764-z>
- Masri, S., & Sassone-Corsi, P. (2018). The emerging link between cancer, metabolism, and circadian rhythms. *Nature Medicine*, 24(12), 1795–1803. <https://doi.org/10.1038/s41591-018-0271-8>
- Gubin, D. G., Weinert, D., Rybina, S. V., Danilova, L. A., Solovieva, S. V., Durov, A. M., Prokopiev, N. Y., & Ushakov, P. A. (2017). Activity, sleep and ambient light have a different impact on circadian blood pressure, heart rate and body temperature rhythms [PMID: 28276854]. *Chronobiology International*, 34(5), 632–649. <https://doi.org/10.1080/07420528.2017.1288632>
- Scheer, F. A. J. L., Hilton, M. F., Mantzoros, C. S., & Shea, S. A. (2009). Adverse metabolic and cardiovascular consequences of circadian misalignment. *Proceedings of the National Academy of Sciences*, 106(11), 4453–4458. <https://doi.org/10.1073/pnas.0808180106>
- Phillips, A. J. K., Clerx, W. M., O'Brien, C. S., Sano, A., Barger, L. K., Picard, R. W., Lockley, S. W., Klerman, E. B., & Czeisler, C. A. (2017). Irregular sleep/wake patterns are associated with poorer academic performance and delayed circadian and sleep/wake timing. *Scientific Reports*, 7(1), 3216. <https://doi.org/10.1038/s41598-017-03171-4>
- Gullo, F., Ponti, G., Tagarelli, A., & Greco, S. (2009). A time series representation model for accurate and fast similarity detection. *Pattern Recognition*, 42(11), 2998–3014. <https://doi.org/https://doi.org/10.1016/j.patcog.2009.03.030>
- Tsai, H.-J., Kuo, T. B., Lin, Y.-C., & Yang, C. C. (2015). The association between prolonged sleep onset latency and heart rate dynamics among young sleep-onset insomniacs and good sleepers. *Psychiatry Research*, 230(3), 892–898. <https://doi.org/https://doi.org/10.1016/j.psychres.2015.11.030>
- Tackenberg, M. C., & Hughey, J. J. (2021). The risks of using the chi-square periodogram to estimate the period of biological rhythms. *PLOS Computational Biology*, 17(1), 1–16. <https://doi.org/10.1371/journal.pcbi.1008567>
- Morris, C. J., Purvis, T. E., Hu, K., & Scheer, F. A. J. L. (2016). Circadian misalignment increases cardiovascular disease risk factors in humans. *Proceedings of the National Academy of Sciences*, 113(10), E1402–E1411. <https://doi.org/10.1073/pnas.1516953113>
- Benedetti, D., Olcese, U., Frumento, P., Bazzani, A., Bruno, S., d'Ascanio, P., Maestri, M., Bonanni, E., & Faraguna, U. (2021). Heart rate detection by fitbit chargehr™: A validation study versus portable polysomnography. *Journal of Sleep Research*, 30(6), e13346. <https://doi.org/https://doi.org/10.1111/jsr.13346>

- Walch, O., Huang, Y., Forger, D., & Goldstein, C. (2019). Sleep stage prediction with raw acceleration and photoplethysmography heart rate data derived from a consumer wearable device. *Sleep*, 42(12), zsz180. <https://doi.org/10.1093/sleep/zsz180>
- Refinetti, R., Cornelissen, G., & Halberg, F. (2007). Procedures for numerical analysis of circadian rhythms. *Biological Rhythm Research*, 38(4), 275–325. <https://doi.org/10.1080/09291010600903692>
- Stucky, B., Clark, I., Azza, Y., Karlen, W., Achermann, P., Kleim, B., & Landolt, H.-P. (2021). Validation of fitbit charge 2 sleep and heart rate estimates against polysomnographic measures in shift workers: Naturalistic study. *J Med Internet Res*, 23(10), e26476. <https://doi.org/10.2196/26476>
- Penzel, T., Kantelhardt, J., Lo, C. C., et al. (2003). Dynamics of heart rate and sleep stages in normals and patients with sleep apnea. *Neuropsychopharmacology*, 28, S48–S53. <https://doi.org/10.1038/sj.npp.1300146>
- Ruf, T. (1999). The Lomb-Scargle periodogram in biological rhythm research: Analysis of incomplete and unequally spaced time-series. *Biological Rhythm Research*, 30(2), 178–201. <https://doi.org/10.1076/brrm.30.2.178.1422>
- McDonnell, E. I., Zipunnikov, V., Schrack, J. A., Goldsmith, J., & Wrobel, J. (2021). Registration of 24-hour accelerometric rest-activity profiles and its application to human chronotypes. *Biological Rhythm Research*, 53(8), 1299–1319. <https://doi.org/10.1080/09291016.2021.1929673>
- Rösler, L., van der Lande, G., Leerssen, J., Vandegriffe, A. G., Lakbila-Kamal, O., Foster-Dingley, J. C., Albers, A. C. W., & van Someren, E. J. W. (2022). Combining cardiac monitoring with actigraphy aids nocturnal arousal detection during ambulatory sleep assessment in insomnia. *Sleep*, 45(5), zsac031. <https://doi.org/10.1093/sleep/zsac031>
- Lunsford-Avery, J. R., Engelhard, M. M., Navar, A. M., & Kollins, S. H. (2018). Validation of the sleep regularity index in older adults and associations with cardiometabolic risk. *Scientific Reports*, 8(1), 14158. <https://doi.org/10.1038/s41598-018-32402-5>
- Snyder, F., Hobson, J. A., Morrison, D. F., & Goldfrank, F. (1964). Changes in respiration, heart rate, and systolic blood pressure in human sleep [PMID: 14174589]. *Journal of Applied Physiology*, 19(3), 417–422. <https://doi.org/10.1152/jappl.1964.19.3.417>
- Whitehurst, L. N., Naji, M., & Mednick, S. C. (2018). Comparing the cardiac autonomic activity profile of daytime naps and nighttime sleep. *Neurobiology of Sleep and Circadian Rhythms*, 5, 52–57. <https://doi.org/10.1016/j.nbscr.2018.03.001>
- Katori, M., Shi, S., Ode, K. L., Tomita, Y., & Ueda, H. R. (2022). The 103,200-arm acceleration dataset in the uk biobank revealed a landscape of human sleep

- phenotypes. *Proceedings of the National Academy of Sciences*, 119(12), e2116729119. <https://doi.org/10.1073/pnas.2116729119>
- Bunde, A., Havlin, S., Kantelhardt, J. W., Penzel, T., Peter, J.-H., & Voigt, K. (2000). Correlated and uncorrelated regions in heart-rate fluctuations during sleep. *Phys. Rev. Lett.*, 85, 3736–3739. <https://doi.org/10.1103/PhysRevLett.85.3736>
- Fudolig, M. I., Bloomfield, L. S., Price, M., Bird, Y. M., Hidalgo, J. E., Kim, J. N., Llorin, J., Lovato, J., McGinnis, E. W., McGinnis, R. S., Ricketts, T., Stanton, K., Dodds, P. S., & Danforth, C. M. (2024). The two fundamental shapes of sleep heart rate dynamics and their connection to mental health in college students. *Digital Biomarkers*, 8(1), 120–131. <https://doi.org/10.159/000539487>
- Mason, I. C., Grimaldi, D., Reid, K. J., Warlick, C. D., Malkani, R. G., Abbott, S. M., & Zee, P. C. (2022). Light exposure during sleep impairs cardiometabolic function. *Proceedings of the National Academy of Sciences*, 119(12), e2113290119. <https://doi.org/10.1073/pnas.2113290119>
- Sateia, M. J. (2014). International classification of sleep disorders-third edition. *CHEST*, 146(5), 1387–1394. <https://doi.org/10.1378/chest.14-0970> doi: 10.1378/chest.14-0970.
- Morin, C. M., Drake, C. L., Harvey, A. G., Krystal, A. D., Manber, R., Riemann, D., & Spiegelhalder, K. (2015). Insomnia disorder. *Nature Reviews Disease Primers*, 1(1), 15026. <https://doi.org/10.1038/nrdp.2015.26>
- Schlagintweit, J., Laharnar, N., Glos, M., et al. (2023). Effects of sleep fragmentation and partial sleep restriction on heart rate variability during night. *Scientific Reports*, 13, 6202. <https://doi.org/10.1038/s41598-023-33013-5>
- Buysse, D. J., Reynolds, C. F., Monk, T. H., Berman, S. R., & Kupfer, D. J. (1989). The pittsburgh sleep quality index: A new instrument for psychiatric practice and research. *Psychiatry Research*, 28(2), 193–213. [https://doi.org/https://doi.org/10.1016/0165-1781\(89\)90047-4](https://doi.org/https://doi.org/10.1016/0165-1781(89)90047-4)
- Johns, M. W. (1991). A new method for measuring daytime sleepiness: The epworth sleepiness scale. *Sleep*, 14(6), 540–545. <https://doi.org/10.1093/sleep/14.6.540>
- Lee, M. P., Kim, D. W., Mayer, C., Walch, O., & Forger, D. B. (2024). The combination of topological data analysis and mathematical modeling improves sleep stage prediction from consumer-grade wearables [PMID: 39552521]. *Journal of Biological Rhythms*, 39(6), 535–553. <https://doi.org/10.1177/07487304241288607>
- de Zambotti, M., Baker, F. C., Willoughby, A. R., Godino, J. G., Wing, D., Patrick, K., & Colrain, I. M. (2016). Measures of sleep and cardiac functioning during sleep using a multi-sensory commercially-available wristband in adolescents.

- Physiology & Behavior*, 158, 143–149. <https://doi.org/https://doi.org/10.1016/j.physbeh.2016.03.006>
- Faust, L., Feldman, K., Mattingly, S. M., Hachen, D., & V. Chawla, N. (2020). Deviations from normal bedtimes are associated with short-term increases in resting heart rate. *npj Digital Medicine*, 3(1), 39. <https://doi.org/10.1038/s41746-020-0250-6>
- Terman, J. S., Terman, M., Lo, E.-S., & Cooper, T. B. (2001). Circadian time of morning light administration and therapeutic response in winter depression. *Archives of General Psychiatry*, 58(1), 69–75. <https://doi.org/10.1001/archpsyc.58.1.69>
- Manjunath, S., Perea, J. A., & Sathyanarayana, A. (2023). Topological data analysis of electroencephalogram signals for pediatric obstructive sleep apnea, 1–4. <https://doi.org/10.1109/EMBC40787.2023.10340674>